Quantum trajectories for propagating Fock states

Ben Q. Baragiola and Joshua Combes

Phys. Rev. A **96**, 023819 — Published 9 August 2017

DOI: 10.1103/PhysRevA.96.023819

Quantum trajectories for propagating Fock states

Ben Q. Baragiola[1,2] and Joshua Combes[2,3,4,5]

[1] *Centre for Engineered Quantum Systems, Macquarie University, NSW 2109, Australia*
[2] *Center for Quantum Information and Control, University of New Mexico 87131, USA*
[3] *Institute for Quantum Computing and Department of Applied Mathematics, University of Waterloo, Waterloo, ON, Canada*
[4] *Perimeter Institute for Theoretical Physics, N2L 2Y5, Canada*
[5] *School of Mathematics and Physics, University of Queensland, Brisbane, QLD, Australia*

(Dated: 27 June 2017)

We derive quantum trajectories (also known as stochastic master equations) that describe an arbitrary quantum system probed by a propagating wave packet of light prepared in a continuous-mode Fock state. We consider three detection schemes of the output light: photon counting, homodyne detection, and heterodyne detection. We generalize to input field states that are superpositions and or mixtures of Fock states and illustrate our formalism with several examples.

I. INTRODUCTION

Propagating wave packets of light prepared with a definite number of photons—Fock states—are well suited for the role of relaying information between nodes of a quantum computing device [1]. In the optical and microwave domains, single-photon fields are routinely produced and manipulated, with ongoing progress toward higher photon numbers [2–4]. Taking advantage of Fock states for quantum technology necessitates a theoretical understanding of their interaction with fundamental quantum components, *e.g.* an atom coupled to a waveguide or a transmon in superconducting circuit QED.

Two useful tools for understanding light-matter interactions are master equations and stochastic master equations. Each is an equation of motion for the reduced state of a quantum system that is coupled to an electromagnetic field. After interacting with the system the field propagates away, carrying with it information. The master equation (ME) is a differential equation for the unconditional reduced system state and ignores any information in the field. The information is not gone; however, and may be retrieved by performing measurements of the output field. A time-continuous measurement of the output fields can be used to find the conditional state of the system, known as a *quantum trajectory* [5, 6]. The equation that takes the sequence of measurement results and determines the system state's conditional evolution is called a stochastic master equation (SME). Different types of field measurement—for instance, direct photon counting or quadrature measurements—yield different SMEs.

The form of an SME depends on the input state of the field. SMEs for Gaussian input fields (vacuum, coherent, thermal, and squeezed) were derived a long time ago [7] and are widely used [8–12]. Due to the inherently nonclassical nature of Fock states, their SMEs have proven more elusive. Propagating Fock states possess temporal correlations which are mapped onto entanglement between system and field as they interact. Consider a single-photon field interacting with a quantum system, see Fig. 1. Classically, two paths have been taken by

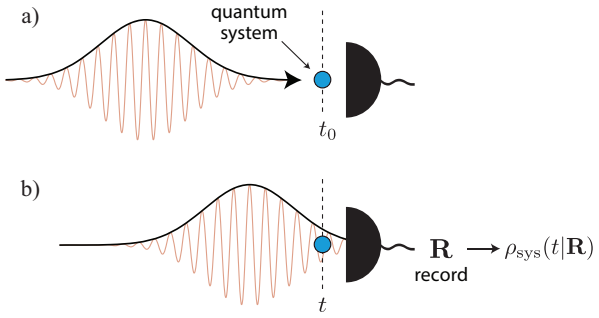

FIG. 1. Depiction of a propagating wave packet interacting with a quantum system followed by measurement of the scattered field. The temporal wave packet is given by a slowly-varying envelope $\xi(t)$ modulating fast oscillations at the carrier frequency. We consider a wave packet prepared in a nonclassical state of definite photon number—a Fock state $|N_\xi\rangle$. a) At time t_0, prior to the interaction, the system and field are unentangled. b) At a later time $t > t_0$, a portion of the wave packet has interacted with the system, and the scattered field has been detected. A quantum trajectory describes the conditional reduced state of the system, $\rho_{\rm sys}(t|\mathbf{R})$, given the measurement record $\mathbf{R}$.

time t: (i) the photon has interacted with the system at some previous time $t' \leq t$, or (ii) the photon has not yet arrived at the system and can be found with certainty in the remaining, future input field $t' > t$. The origin of system-field entanglement is the superposition of these options. This is a departure from the typically considered situation for open quantum systems where the input field at time t is uncorrelated both with the system and with the field at all other times.

In this article we derive stochastic master equations for an arbitrary quantum system probed with a propagating Fock state. The temporal correlations in the input field and the entanglement between the system and field are accounted for with a set of coupled equations. We consider three different detection schemes of the output light: photon counting, homodyne detection of an arbitrary quadrature, and heterodyne detection. We extend our derivation to include input fields in superpositions or

mixtures of Fock states and to inefficient measurements of the field.

Previously some aspects of our theory have been developed. The unconditional MEs for one- and two-photon input fields were introduced by Gheri *et al.* [13] and later extended to many photons in the Fock-state MEs of Baragiola *et al.* [14]. A step towards Fock-state SMEs was given by Gheri *et al.* [13], where they suggested enlarging the Hilbert space to include the source of a single photon using a cascaded approach [15, 16]. The SMEs for input fields containing any superposition or mixture of vacuum and a single photon were given by Gough *et al.* [17, 18]. Recently, various mathematical techniques have extended these results to SMEs for multiphoton input fields [19] and for a class of continuous matrix-product states that includes time-ordered, multiphoton states [20]. These derivations proceed in the Heisenberg picture and rely on mathematical techniques unfamiliar to the physics community. In contrast we provide a Schrödinger-picture derivation, based on the temporal structure of propagating Fock states, that generalizes the Wiseman-Milburn techniques [7, 8]. Our approach gives insight into the physical significance of the equations, provides solid footing for useful generalizations, and enables SMEs for any state of the field in a given temporal mode.

This article is organized as follows. In Sec. II we present the physical model for the interaction of a quantum system with a continuous-mode field using input-output formalism. The properties of Fock states are summarized with an emphasis on a *temporal decomposition* of the field, and a formal description of continuous field measurements and quantum trajectories is given. In Sec. III we present the main results of this article: the stochastic master equations for quantum systems probe by continuous-mode Fock states when the output fields are subject to three types of measurement: photon counting, homodyne detection, and heterodyne detection. In Sec. IV we generalize the SMEs to superpositions and mixtures of Fock states and show how to model imperfect detection and add additional decoherence. As a pedagogical example, we analyze conditional dynamics of a two-level atom in Sec. V. Finally, we summarize our results and provide outlook in Sec. VI.

II. PHYSICAL MODEL AND FORMALISM

A. System-field interaction: input-output theory

A quantum system interacting with a traveling field naturally calls for a formulation in the time domain due to the local-in-time nature of the interaction and measurements. Input-output theory and the underlying continuous-mode quantization of the field provide such a description [8, 21]. Input-output theory is often formulated for an effectively one-dimensional electromagnetic field, such as arises for one-sided cavities [21], photonic waveguides [22, 23], transmission lines in circuit QED [24], and paraxial free-space fields [25], although this is not a necessary restriction [26]. Within this formalism, enforcement of the weak-coupling limit, the Markov approximation, and the rotating wave approximation yields a quantum stochastic differential equation (QSDE) for the time evolution operator that governs unitary system-field dynamics [25, 27].

Consider a one-dimensional, continuous-mode field described by bosonic operators satisfying $[b(\omega), b^\dagger(\omega')] = \delta(\omega - \omega')$. For quasi-monochromatic excitations, *i.e.* when the spectral bandwidth is much smaller than the carrier frequency $\Delta\omega \ll \omega_c$, we define slowly varying, Fourier-transformed field operators [28],

$$b(t) \equiv \frac{1}{\sqrt{2\pi}} \int_{-\infty}^{\infty} d\omega\, b(\omega) e^{-i(\omega-\omega_c)t}. \tag{1}$$

They satisfy the commutation relations $[b(t), b^\dagger(t')] = \delta(t - t')$ and are often referred to as white-noise operators, akin to classical white noise, which is δ-correlated in time. Here, t is a label for the mode of the field that interacts with the system at time t. Due to the singular nature of $b(t)$ and $b^\dagger(t)$, it is often preferable to work with the *quantum noise increments* over an infinitesimal time interval $[t, t + dt)$:

$$dB_t = \int_t^{t+dt} ds\, b(s), \quad dB_t^\dagger = \int_t^{t+dt} ds\, b^\dagger(s), \tag{2a}$$

$$d\Lambda_t = \int_t^{t+dt} ds\, b^\dagger(s) b(s). \tag{2b}$$

In the interval $[t, t + dt)$ the operators dB_t and $dB_t^\dagger$ are infinitesimal annihilation and creation operators, and $d\Lambda_t$ is the infinitesimal number operator. The increments act nontrivially only on $[t, t + dt)$, *e.g.*

$$dB_t = I_{[0,t)} \otimes dB_{[t,t+dt)} \otimes I_{[t+dt,\infty)}, \tag{3}$$

where the interval $[0, t)$ represents the past Hilbert space of the field (the output field), the infinitesimal interval $[t, t + dt)$ the field presently interacting with the system, and the interval $[t + dt, \infty)$ the future field. The rules for taking products of the quantum noise increments are given by the Itō table [21],

$$\begin{aligned} dB_t dB_t^\dagger &= dt, \;\; dB_t d\Lambda_t = dB_t, \\ d\Lambda_t d\Lambda_t &= d\Lambda_t, \;\; d\Lambda_t dB_t^\dagger = dB_t^\dagger, \end{aligned} \tag{4}$$

with all other products vanishing to order dt.

Over the infinitesimal time interval $[t, t + dt)$, the time evolution operator [21, 29],

$$\begin{aligned} U_t =& I_{\rm sys} \otimes I_t - dt\big(iH_{\rm sys} + \tfrac{1}{2}L^\dagger L\big) \otimes I_t \\ & - L^\dagger S \otimes dB_t + L \otimes dB_t^\dagger + (S - I_{\rm sys}) \otimes \Lambda_t, \end{aligned} \tag{5}$$

describes the unitary coupling of the field operators, Eq. (2), to system operators $H_{\rm sys}$, L, and S, which are

determined from the Hamiltonian governing the underlying physical system [30, 31]. From this interaction, the output relations for the quantum noise increments are [32, 33],

$$dB_t^{\text{out}} = dtL \otimes I_t + S \otimes dB_t, \tag{6a}$$

$$d\Lambda_t^{\text{out}} = dtL^\dagger L \otimes I_t + L^\dagger S \otimes dB_t + S^\dagger L \otimes dB_t^\dagger + I_{\text{sys}} \otimes d\Lambda_t. \tag{6b}$$

These are the standard input-output relations [8, 21, 34] with the additional inclusion of the scattering operator S. Each relation is the coherent sum of two contributions: the free field and system scattering.

B. Continuous-mode Fock states

Quasi-monochromatic, continuous-mode fields have a convenient description in terms of the input operators of Eq. (1) [35]. The utility of this description becomes evident when one considers that interactions, Eq. (5), and measurements are local in time. The continuous-mode field is represented in a continuous temporal tensor-product space, $\mathcal{H}_{\text{field}} = \bigotimes_i \mathcal{H}_{t_i}$, where $\mathcal{H}_{t_i}$ is the Hilbert space associated with the field at time t_i [25]. The statistics of field states that factorize with respect to a given time t,

$$|\Psi\rangle = |\Psi_{t)}\rangle \otimes |\Psi_{[t}\rangle, \tag{7}$$

are specified independently on each time interval–the *past* $[t_0, t)$ and the *future* $[t, \infty)$. Field states that factorize temporally with respect to *all* times are described by a temporal tensor-product state,

$$|\Psi\rangle = \bigotimes_i |\Psi_{t_i}\rangle, \tag{8}$$

whose statistics can be independently specified over any time interval. Critical to the derivation of a master equation or SME is whether the input field is described by a temporal tensor-product state.

The elementary continuous-mode state is vacuum, given by the product state,

$$|\mathbf{0}\rangle \equiv \bigotimes_i |0_{t_i}\rangle = |0\rangle \otimes |0\rangle \otimes \ldots, \tag{9}$$

indicating vacuum at every time. From continuous-mode vacuum, continuous-wave coherent states are constructed by displacing each vacuum component in $|\mathbf{0}\rangle$ to the same amplitude; $|\alpha\rangle = \bigotimes_i |\alpha_{t_i}\rangle$ [35].

Field states that do not factorize in time are inherently nonstationary and further can possess temporal correlations. We now construct normalized, nonstationary continuous-mode fields in a single temporal mode, with particular emphasis on propagating Fock states. Consider a quasi-monochromatic field in temporal mode $\tilde{\xi}(t) = \xi(t)e^{i\omega_c t}$. Rapid oscillations at the carrier frequency ω_c are modulated by a slowly varying wave packet $\xi(t)$ that is square-normalized,

$$\int ds |\xi(s)|^2 = 1. \tag{10}$$

Field states are constructed in the temporal mode $\xi(t)$ by the wave packet creation operator [35],

$$B^\dagger(\xi) \equiv \int ds\, \xi(s) b^\dagger(s), \tag{11}$$

which satisfies $[B(\xi), B^\dagger(\xi)] = 1$. For example, a wave-packet coherent state with time-varying amplitude $\alpha(t) = \alpha_0 \xi(t)$, for complex peak amplitude α_0, is generated from vacuum by a continuous-mode displacement operator: $|\alpha_\xi\rangle = D[\alpha(t)]|\mathbf{0}\rangle = \exp[\alpha_0^* B^\dagger(\xi) - \alpha_0 B(\xi)]|\mathbf{0}\rangle$ [35].

A propagating single photon in the wave packet $\xi(t)$ is generated by applying the wave packet creation operator, Eq. (11), directly to continuous-mode vacuum [13, 35], $|1_\xi\rangle = B^\dagger(\xi)|\mathbf{0}\rangle$. This can be interpreted as superposition of photon creation times weighted by $\xi(t)$ [35–37]. A straightforward extension provides the definition of continuous-mode Fock states (referred to hereafter as *Fock states*) with n photons [14, 35],

$$|n_\xi\rangle = \tfrac{1}{\sqrt{n!}} \left[B^\dagger(\xi)\right]^n |\mathbf{0}\rangle, \tag{12}$$

satisfying $\langle n_\xi | n_\xi \rangle = 1$. The action of the quantum noise increments in Eq. (2) on Fock states is [14]

$$dB_t |n_\xi\rangle = dt\sqrt{n}\xi(t)|n-1_\xi\rangle \tag{13}$$

$$d\Lambda_t |n_\xi\rangle = dB_t^\dagger \sqrt{n}\xi(t)|n-1_\xi\rangle. \tag{14}$$

1. Temporal decomposition

Shortly we consider the interaction of Fock states with an arbitrary quantum system. These interactions are time-local [Eq. (5)], so it is convenient to perform a *temporal decomposition* of the field state. That is, we write the input Fock state in a basis where its projection on the time of interaction is made explicit. This is achieved by decomposing the wave-packet creation operator, $B^\dagger(\xi)$, into three intervals—the past $[t_0, t)$, the current $[t, t+dt)$, the future $[t+dt, \infty)$. The current interval is infinitesimal, such that the probability of detecting two photons simultaneously is vanishingly small [8, 38, 39] (equivalent to $dB_t^\dagger dB_t^\dagger = 0$ in the Itō table). With respect to this decomposition, the wave-packet creation operator in Eq. (11) is,

$$B^\dagger(\xi) = \underbrace{\int_{t_0}^{t} ds\, \xi(s) b^\dagger(s)}_{\equiv B_{t)}^\dagger(\xi)} + \xi(t) dB_t^\dagger + \underbrace{\int_{t+dt}^{\infty} ds\, \xi(s) b^\dagger(s)}_{\equiv B_{[t+dt}^\dagger(\xi)}, \tag{15}$$

where $B^\dagger_{t)}(\xi)$ and $B^\dagger_{[t+dt}(\xi)$ create photons in the *past* and *future* with respect to t. We have used abbreviated interval notation, $[t_0, t) \to t)$ and $[t, \infty) \to [t$. Each portion of the wave packet creation operator in Eq. (15) acts on a different interval of multimode vacuum,

$$|\mathbf{0}\rangle = |0_{t)}\rangle \otimes |0_t\rangle \otimes |0_{[t+dt}\rangle, \tag{16}$$

where $|0_t\rangle$ is the infinitesimal vacuum at the current time interval. Applying Eq. (15) to this decomposition of the vacuum we obtain a temporal decomposition of the single-photon wave packet:

$$\begin{aligned}|1_\xi\rangle =& |1_{t)}\rangle \otimes |0_t\rangle \otimes |0_{[t+dt}\rangle + \sqrt{dt}\xi(t)|0_{t)}\rangle \otimes |1_t\rangle \otimes |0_{[t+dt}\rangle \\ &+ |0_{t)}\rangle \otimes |0_t\rangle \otimes |1_{[t+dt}\rangle,\end{aligned} \tag{17}$$

where the infinitesimal single-photon state in the current time interval is [8]

$$|1_t\rangle = \frac{dB^\dagger_t}{\sqrt{dt}}|0_t\rangle. \tag{18}$$

Inserting Eq. (15) into the definition of a Fock state in Eq. (12) gives the temporal decomposition,

$$|n_\xi\rangle = \tfrac{1}{\sqrt{n!}}\left[B^\dagger_{t)}(\xi) + \xi(t)dB^\dagger_t + B^\dagger_{[t+dt}(\xi)\right]^n|\mathbf{0}\rangle. \tag{19}$$

Further details about the temporal decomposition of Fock states can be found in Appendix A.

A basis for an infinitesimal interval $[t, t+dt)$ can be constructed from the infinitesmal states $|0_t\rangle$ and $|1_t\rangle$ [39, Sec. V A]. A relative-state decomposition of an n-photon Fock state in this basis yields,

$$|n_\xi\rangle = |0_t\rangle\langle 0_t|n_\xi\rangle + |1_t\rangle\langle 1_t|n_\xi\rangle \tag{20a}$$

$$= |0_t\rangle \otimes |\overline{n}_\xi\rangle + \sqrt{n\,dt}\xi(t)|1_t\rangle \otimes |\overline{n-1}_\xi\rangle, \tag{20b}$$

which can also be found by expanding Eq. (19), as shown in Appendix A. The state $|\overline{n}_\xi\rangle$ is the partial projection of a Fock state onto infinitesimal vacuum,

$$|\overline{n}_\xi\rangle \equiv \langle 0_t|n_\xi\rangle. \tag{21}$$

By taking the inner product of Eq. (20) with itself we relate the inner product of $|\overline{n}_\xi\rangle$ to the original wave packet

$$\langle\overline{n}_\xi|\overline{n}_\xi\rangle = 1 - ndt|\xi(t)|^2\langle\overline{n-1}_\xi|\overline{n-1}_\xi\rangle \tag{22a}$$

$$= 1 - ndt|\xi(t)|^2, \tag{22b}$$

where, in the second line we used $\langle\overline{n-1}_\xi|\overline{n-1}_\xi\rangle = 1 - (n-1)dt|\xi(t)|^2\langle\overline{n-2}_\xi|\overline{n-2}_\xi\rangle$, and kept terms to order dt.

C. Continuous measurement of the field

After the system and field interact and become entangled the output field is measured. Continuous-time measurements are described by a time-ordered sequence of infinitesimal measurements collected as the field impinges on the detection apparatus. The infinitesimal time interval is short enough that the probability of detecting two photons is negligible; other situations are obtained by integrating over time. In an infinitesimal interval, a projective measurement with outcome R is described by the partial projector,

$$\Pi_R = I_{t)} \otimes |R_t\rangle\langle R_t| \otimes I_{[t+dt}, \tag{23}$$

where $|R_t\rangle = a_R|0_t\rangle + b_R|1_t\rangle$ with $|a_R|^2 + |b_R|^2 = 1$. The partial projector in Eq. (23) and its complement act nontrivially only on the infinitesimal interval where the measurement is performed, $[t, t+dt)$. Together they constitute a two-outcome POVM that resolves the identity on the infinitesimal Fock space, $\sum_R \Pi_R = I_{t)} \otimes I_t \otimes I_{[t+dt} = I_{\text{field}}$.

A sequence of such infinitesimal measurements over a time interval $[t_0, t)$ comprises a continuous measurement. The collection of measurement results $\mathbf{R}$, referred to as the measurement record, is described by a partial projector,

$$\Pi_{\mathbf{R}} = |\mathbf{R}\rangle\langle\mathbf{R}| \otimes I_{[t}, \tag{24}$$

where $|\mathbf{R}\rangle$ is a tensor product of infinitesimal projective eigenstates, as in Eq. (23),

$$|\mathbf{R}\rangle = |R_{[t-dt,t)}\rangle \otimes \cdots \otimes |R_{[t_0,t_0+dt)}\rangle = \bigotimes_{t_i}|R_{t_i}\rangle. \tag{25}$$

The partial projectors resolve the identity over the time interval $[t_0, t)$,

$$\int d\mathbf{R}\,|\mathbf{R}\rangle\langle\mathbf{R}| = I_{t)}, \tag{26}$$

and, with Eq. (24), over the full Fock space [39, Sec. V]. Regardless of the specific record $\mathbf{R}$, the measured portion of the field becomes disentangled from the the future field.

D. Quantum trajectories

Consider a quantum system interacting with a continuous-mode field in an initially unentangled joint state,

$$\rho_{\text{joint}}(t_0) = \rho_0 \otimes |\Psi\rangle\langle\Psi|, \tag{27}$$

where ρ_0 is the initial system state and $|\Psi\rangle$ the initial field state. The time evolution operator that entangles the system and field in each infinitesimal time interval $[t, t+dt)$ has the general form given in Eq. (5). The total time evolution from initial time t_0 to time t is given by the time-ordered product of infinitesimal unitaries,

$$\begin{aligned}U(t_0, t) &= U(t-dt, t)\cdots U(t_0, t_0+dt) \\ &= \overleftarrow{\prod_s} U(s, s+dt).\end{aligned} \tag{28}$$

Through unitary interaction alone, the entangled joint state of the system and field at time t is given by

$$\rho_{\text{joint}}(t) = U(t_0,t)\rho_{\text{joint}}(t_0)U^\dagger(t_0,t). \tag{29}$$

When measurements are performed on the output field, the joint state is conditioned on the random measurement outcomes. For a measurement record $\mathbf{R}$ described by the projector in Eq. (24), the conditional joint state is found with the usual measurement update rule

$$\rho_{\text{joint}}(t|\mathbf{R}) = \frac{|\mathbf{R}\rangle\langle\mathbf{R}|U(t_0,t)\rho_{\text{joint}}(t_0)U^\dagger(t_0,t)|\mathbf{R}\rangle\langle\mathbf{R}|}{\Pr(\mathbf{R})}, \tag{30}$$

where $\Pr(\mathbf{R})$ is the probability of obtaining $\mathbf{R}$. It will become useful to describe this quantum operation on the joint state with a *conditional evolution operator* $C_{\mathbf{R}}$ that includes the interaction $U(t_0,t)$ and measurements $|\mathbf{R}\rangle$ on the interval $[t_0,t)$,

$$C_{\mathbf{R}} \equiv \langle\mathbf{R}|U(t_0,t)\otimes I_{[t}. \tag{31}$$

Then, Eq. (30) can be written

$$\rho_{\text{joint}}(t|\mathbf{R}) = \frac{C_{\mathbf{R}}\rho_{\text{joint}}(t_0)C_{\mathbf{R}}^\dagger}{\Pr(\mathbf{R})}\otimes|\mathbf{R}\rangle\langle\mathbf{R}|, \tag{32}$$

with probability given by

$$\Pr(\mathbf{R}) = \text{Tr}\big[C_{\mathbf{R}}^\dagger C_{\mathbf{R}}\rho_{\text{joint}}(t_0)\big]. \tag{33}$$

We note that in many physical situations the measured portion of the field is destroyed by the detection process. Destructive measurements can be obtained by tracing over the past field in Eq. (30), leaving only a classical measurement record and the future input field.

Jack and Collett employed a joint-state description similar to Eq. (30) to study non-Markovian light-matter interactions [39]. While it provides the full, conditional joint state, such a description is difficult to evaluate in practice due to the immense Hilbert space of the continuous-mode field. Here, we present an alternate approach and focus on the reduced system state,

$$\rho_{\text{sys}}(t) = \text{Tr}_{\text{field}}[\rho_{\text{joint}}(t)], \tag{34}$$

as the field is continuously measured. Note that from Eq. (34) forward, we use simplified notation that does explicitly refer to the entire measurement record $\mathbf{R}$, except when necessary.

Typically a stochastic master equation (SME), or *quantum trajectory*, is a way to write the the evolution of the reduced system state as the solution to a stochastic differential equation [5]:

$$d\rho_{\text{sys}}(t) = \frac{\bar{\rho}_{\text{sys}}(t+dt|R_t)}{\Pr(R_t)} - \rho_{\text{sys}}(t). \tag{35}$$

The primary mathematical objects in the derivation of SMEs are the *Kraus operators* $M_R = \langle R_t|U(t,t+dt)|\psi_{\text{field}}\rangle$. Given measurement result R_t, the Kraus operators provide a method for the explicit calculation of the unnormalized conditional state above,

$$\bar{\rho}_{\text{sys}}(t+dt|R_t) = M_R\rho_{\text{sys}}(t)M_R^\dagger, \tag{36}$$

and the probability of outcome R_t,

$$\Pr(R_t) = \text{Tr}\big[M_R^\dagger M_R\rho_{\text{sys}}(t)\big], \tag{37}$$

which normalizes the state. The reduced-state dynamics are Markovian when the input field factorizes temporally with respect to the interaction and measurements, *e.g.* vacuum and coherent states. In this case, the map for the reduced state from time t to $t+dt$, Eq. (36), is entirely specified by the joint state at time t, the entangling unitary [Eq. (5)], and the measurement result in that interval, R_t.

For input fields that do not admit a temporal tensor-product factorization, such as continuous-mode propagating Fock states (Sec. II B), the reduced-system dynamics are manifestly non-Markovian, and the SME cannot be written in the form of Eq. (35). The major result of this manuscript is a technique to generalize this SME to the case of propagating Fock-state input fields, which we present in Sec. III.

III. FOCK-STATE STOCHASTIC MASTER EQUATIONS

We are now equipped to tackle the primary focus of this manuscript—conditional dynamics for a quantum system probed by a continuous-mode, propagating Fock state. Our approach uses a set of coupled stochastic master equations. Their derivation follows from an extension of the standard approach to deriving SMEs in the Schrödinger-picture, which begins by identifying the Kraus operators for infinitesimal measurements of the field [8].

In Sec III A we describe the mathematical objects that arise in the derivation. In the subsections that follow we derive the SMEs for photon counting, homodyne, and heterodyne measurements. In each section, we state the result and then provide the derivation for interested readers. The Heisenberg-picture formulation of the Fock-state SMEs is given in Appendix B.

A. Structure of the SMEs

We begin with a quantum system and input field in the joint state

$$\rho_{\text{joint}}(t_0) = \rho_0\otimes|N_\xi\rangle\langle N_\xi|, \tag{38}$$

with the system initially in state ρ_0 and the field described by a propagating N-photon Fock state $|N_\xi\rangle$, given by Eq. (12). As the wave packet arrives, the system

and field become entangled by the infinitesimal unitary, Eq. (5). Then, the output portion of the field is measured. For arbitrary time t the joint state of the system and field is formally given by Eq. (30), and the reduced system state by

$$\rho_{\rm sys}(t) = \frac{1}{\Pr(\mathbf{R})}\mathrm{Tr}_{\rm field}\left[C_{\mathbf{R}}\rho_0 \otimes |N_\xi\rangle\langle N_\xi| C_{\mathbf{R}}^\dagger\right]. \tag{39}$$

We show below that the SME for the reduced system state $\rho_{\rm sys}(t)$ couples to a family of density-matrix-like operators,

$$\rho_{m,n}(t) \equiv \frac{1}{\Pr(\mathbf{R})}\mathrm{Tr}_{\rm field}\left[C_{\mathbf{R}}\rho_0 \otimes |m_\xi\rangle\langle n_\xi| C_{\mathbf{R}}^\dagger\right] \tag{40}$$

for $0 \leq \{m,n\} \leq N$. These operators represent fixed photon-number subspaces and coherences between them. Clearly, for N-photon Fock-state input the reduced system state is given by the top-level equation: $\rho_{\rm sys}(t) = \rho_{N,N}(t)$. The operators $\rho_{m,n}(t)$, which have the same Hilbert-space dimension as $\rho_{\rm sys}(t)$, first arose in the single- and two-photon master equations of Gheri et al. [13] and reappeared for conditional and unconditional reduced-state dynamics in a variety of settings [14, 17–19]. Their initial conditions ($C_{\mathbf{R}} = I$) are

$$\rho_{m,n}(t_0) = \mathrm{Tr}_{\rm field}\left[\rho_0 \otimes |m_\xi\rangle\langle n_\xi|\right] = \delta_{m,n}\rho_0. \tag{41}$$

That is, the diagonal operators ($m = n$) are initialized to the system state ρ_0. The off-diagonal operators ($m \neq n$) are initially zero, are traceless at all times, and satisfy $\rho_{m,n}(t) = \rho_{n,m}^\dagger(t)$ [13, 14].

The field trace in the definition of $\rho_{m,n}(t)$ can be explicitly taken to find the formal quantum operation described by Eq. (40). At time t, the past portion of the field has interacted with the system and subsequently been measured while the future portion of the field has not. We show in Appendix A the decomposition of an input Fock state into a future and past basis of Fock states with respect to a chosen time t. These are defined over two disjoint temporal modes which together comprise the initial wave packet mode. For a field that has been detected up to time t, the field trace can be formally taken using the (normalized) Fock basis over the future wave packet, $|n_{[t}\rangle$,

$$\rho_{m,n}(t) = \frac{1}{\Pr(\mathbf{R})}\sum_{n'=0}^{\infty}\Omega_{\mathbf{R}}^{m,n'}\rho_0\left(\Omega_{\mathbf{R}}^{n,n'}\right)^\dagger, \tag{42}$$

where the Kraus operators are

$$\Omega_{\mathbf{R}}^{m,n'} = \langle n'_{[t}|C_{\mathbf{R}}|m_\xi\rangle = \left(\langle n'_{[t}| \otimes \langle \mathbf{R}|\right)U(t_0,t)|m_\xi\rangle. \tag{43}$$

Our derivation here does not require these full Kraus operators, but we introduce the machinery here for completeness, noting that it will be used in future work to illustrate system-field correlations.

In the Fock-state SME derivations that follow, the unnormalized operators,

$$\bar{\rho}_{m,n}(t+dt|R_t) = \frac{1}{\Pr(\mathbf{R})}\mathrm{Tr}_{\rm field}\left[\mathcal{M}_R^m(t)\rho_0\mathcal{M}_R^{n\dagger}(t)\right], \tag{44}$$

are updated in each infinitesimal interval with a quantum operation described by the Fock-state *pseudo* Kraus operators, $\mathcal{M}_R^n(t)$, defined for each input photon number n as indicated by the superscript. These are found by amending $C_{\mathbf{R}}$ to include the additional conditional dynamics on the current time interval, given by U_t and $|R_t\rangle$, and then acting on an input Fock state $|n_\xi\rangle$:

$$\mathcal{M}_R^n(t) \equiv \langle R_t|U_t C_{\mathbf{R}}|n_\xi\rangle. \tag{45}$$

The pseudo Kraus operators are distinct from the Kraus operators, Eq. (43), because they still have support on the Hilbert space of the future field. However, we will make judicious use of $\mathcal{M}_R^n(t)$ in the following derivations of the Fock-state SMEs, and for simplicity we henceforth refer to them as the Fock-state Kraus operators.

In the derivations below, we show that the $\rho_{m,n}(t)$ couple amongst themselves and form a closed, Markovian set of equations which can be solved to ultimately find $\rho_{\rm sys}(t)$. The differential equations have the form

$$d\rho_{m,n}(t|R_t) = \frac{\bar{\rho}_{m,n}(t+dt|R_t)}{\Pr(R_t)} - \rho_{m,n}(t), \tag{46}$$

where, importantly, each $d\rho_{m,n}(t)$ is a function only of $\rho_{m,n}(t)$, $\rho_{m-1,n}(t)$, $\rho_{m,n-1}(t)$, and $\rho_{m-1,n-1}(t)$ for $m,n \geq 0$. The lowest level equation ($m = n = 0$) for $d\rho_{0,0}(t)$ closes and is only a function of $\rho_{0,0}(t)$ [40]. As $\rho_{m,n}(t) = \rho_{n,m}^\dagger(t)$, there are at most $\frac{1}{2}(N+1)(N+2)$ independent equations [14].

The probability of obtaining the infinitesimal measurement outcome R_t is given by the conditional expectation value of the infinitesimal projector, Eq. (23), with respect to the joint state. Using the Fock-state Kraus operators, it can be written as

$$\Pr(R_t) = \frac{1}{\Pr(\mathbf{R})}\mathrm{Tr}\left[\mathcal{M}_R^{N\dagger}(t)\mathcal{M}_R^N(t)\rho_0\right], \tag{47}$$

for an initial N-photon Fock state. Note that in Eq. (46) all the $\rho_{m,n}(t)$ are rescaled by Eq. (47) for a given measurement outcome. The result is that only the top-level matrix $\rho_{N,N}(t)$, which is indeed the physical reduced state $\rho_{\rm sys}(t)$, remains normalized to unit trace, while the traces of other $\rho_{m,n}(t)$ may vary.

The Fock-state SMEs are found by careful manipulation of Eq. (44) and of the measurement probability, Eq. (47), such that both can be written entirely in terms of the operators $\rho_{m,n}(t)$. Then Eq. (46) describes a closed set of coupled equations that can be solved, and the physical reduced state, Eq. (40), extracted. Below, we go through this derivation in detail for the Fock-state photon-counting SME.

B. Fock-state photon-counting SME

We begin with the photon-counting SME for a quantum system probed by an N-photon Fock state. After interacting with the quantum system, the output fields are sent to a photodetector. Let $N(t)$ denote the number of photons detected up to time t. In the interval $[t, t+dt)$ the random variable dN counts the number of photons, with at most one photon detected. Thus, dN has outcomes 0 (vacuum detection) and 1 (photon detection). The conditional evolution under continuous photon counting is given by the set of coupled SMEs,

$$\begin{aligned} d\rho_{m,n}(t) = \\ dt\Big(-i[H_{\rm sys},\rho_{m,n}] - \tfrac{1}{2}\big\{L^\dagger L,\rho_{m,n}\big\}_+ - \sqrt{m}\xi(t)L^\dagger S\rho_{m-1,n} - \sqrt{n}\xi^*(t)\rho_{m,n-1}S^\dagger L - \sqrt{mn}|\xi(t)|^2\rho_{m-1,n-1}\Big) + \Pr(J)\rho_{m,n} \\ + dN\left(\frac{L\rho_{m,n}L^\dagger + \sqrt{m}\xi(t)S\rho_{m-1,n}L^\dagger + \sqrt{n}\xi^*(t)L\rho_{m,n-1}S^\dagger + \sqrt{mn}|\xi(t)|^2 S\rho_{m-1,n-1}S^\dagger}{\Pr(J)/dt} - \rho_{m,n}\right), \end{aligned} \tag{48}$$

where the $\rho_{m,n}$ are defined in Eq. (40) (henceforth we suppress the argument t, except where necessary), for $m,n \in \{0,...,N\}$. The reduced system state is given at all times by the top-level equation, $\rho_{\rm sys} = \rho_{N,N}$, whose evolution is tied to that of other operators $\rho_{m,n}$. The initial conditions for $\rho_{m,n}$ are given by Eq. (41). Conditional expectation values of system operators are taken with respect to the reduced system state as usual; *e.g.* $\mathbb{E}[X(t)|\mathbf{R}] = \mathrm{Tr}[X\rho_{\rm sys}(t)]$.

The probability of detecting a photon, the "jump" probability, in the time interval $[t, t+dt)$ is

$$\begin{aligned} \Pr(J) =& dt\,\mathrm{Tr}\big[L^\dagger L\rho_{N,N} + \sqrt{N}\xi(t)L^\dagger S\rho_{N-1,N} \\ &+ \sqrt{N}\xi^*(t)S^\dagger L\rho_{N,N-1} + N|\xi(t)|^2\rho_{N-1,N-1}\big]. \end{aligned} \tag{49}$$

This probability is, in fact, the conditional expectation value of the infinitesimal output photon number operator Eq. (7), $\mathbb{E}[d\Lambda_t^{\rm out}|\mathbf{R}]$. Here, we use the notation $\Pr(J)$ with the implicit understanding that the jump probability is conditional and depends on the prior measurement record $\mathbf{R}$. The detection probability, Eq. (49), is a result of photons radiating from the system (first term), photons in the free field (last term), and interference between the two (remaining terms). It is important to note that the trace of $\rho_{N-1,N-1}$, or indeed of any $\rho_{m,n}$ other than the reduced system state $\rho_{\rm sys}$, is not constrained to be equal to 1 [41].

One can also write Eq. (48) in an alternate form,

$$\begin{aligned} d\rho_{m,n}(t) =& dt\,\mathcal{L}_{m,n}[\mathbf{G},\xi(t)] \\ &+ d\mathcal{J}_C(t)\left(\frac{L\rho_{m,n}L^\dagger + \sqrt{m}\xi(t)S\rho_{m-1,n}L^\dagger + \sqrt{n}\xi^*(t)L\rho_{m,n-1}S^\dagger + \sqrt{mn}|\xi(t)|^2 S\rho_{m-1,n-1}S^\dagger}{\Pr(J)/dt} - \rho_{m,n}\right), \end{aligned} \tag{50}$$

where

$$d\mathcal{J}_C(t) \equiv dN - \Pr(J), \tag{51}$$

is called the *photon-counting innovations*. We have grouped the system operators into the operator-triple, $\mathbf{G} = \{S, L, H_{\rm sys}\}$, and introduced $\mathcal{L}_{m,n}[\mathbf{G},\xi(t)]$, which is shorthand notation for a superoperator that acts on a set of $\rho_{m,n}$ operators as follows:

$$\begin{aligned} \mathcal{L}_{m,n}[\mathbf{G},\xi(t)] \equiv& -i[H_{\rm sys},\rho_{m,n}] + \mathcal{D}_L[\rho_{m,n}] \\ &+ \sqrt{m}\xi(t)[S\rho_{m-1,n}, L^\dagger] \\ &+ \sqrt{n}\xi^*(t)[L,\rho_{m,n-1}S^\dagger] \\ &+ \sqrt{mn}|\xi(t)|^2\big(S\rho_{m-1,n-1}S^\dagger - \rho_{m-1,n-1}\big), \end{aligned} \tag{52}$$

where the Lindblad superoperator is

$$\mathcal{D}_L[\rho] \equiv L\rho L^\dagger - \tfrac{1}{2}(L^\dagger L\rho + \rho L^\dagger L). \tag{53}$$

Equation (52) is simply the unconditional part of the evolution—that is, the Fock-state master equations derived in Ref. [14].

1. *Derivation*

The joint system-field state is initialized at t_0 in the unentangled state given by Eq. (38). At a later time $t > t_0$, continuous photon counting has generated a measurement record $\mathbf{R}$. The projectors for photon counting in

an infinitesimal time interval are constructed from eigenstates of the infinitesimal photon-number operator $d\Lambda_t$. Using Carmichael's notation [5, 6] we label the infinitesimal outcomes as $R_t \in \{\emptyset, J\}$, describing either vacuum or a single photon, respectively. These correspond to eigenstates $|0_t\rangle$ and $|1_t\rangle$ [Eq. (18)] with respective eigenvalues $\{0, 1\}$. The associated infinitesimal measurement projectors, Eq. (23), are

$$\Pi_\emptyset = I_{t)} \otimes |0_t\rangle\langle 0_t| \otimes I_{[t+dt}, \tag{54a}$$
$$\Pi_J = I_{t)} \otimes |1_t\rangle\langle 1_t| \otimes I_{[t+dt}. \tag{54b}$$

The conditional joint state, Eq. (30), is subject to entangling interaction and measurement in the infinitesimal time interval $[t, t+dt)$. Our task now is to find the reduced physical state and associated unnormalized operators $\bar{\rho}_{m,n}$, given by Eq. (44), for each of the two outcomes in that interval.

We begin with the case of vacuum detection ($R_t = \emptyset$). The vacuum Kraus operators from Eq. (45) are of the form

$$\mathcal{M}^n_\emptyset(t) = \langle 0_t|U_t C_{\mathbf{R}}|n_\xi\rangle. \tag{55}$$

We insert the entangling unitary, Eq. (5), and use the relative state decompostion of the input field with respect to the current time, Eq. (20), and find

$$\begin{aligned}\mathcal{M}^n_\emptyset(t) =& \big[I_{\rm sys} - dt\big(iH_{\rm sys} + \tfrac{1}{2}L^\dagger L\big)\big] C_{\mathbf{R}}|\overline{n}_\xi\rangle \\ &- dt\sqrt{n}\xi(t)L^\dagger S C_{\mathbf{R}}|\overline{n-1}_\xi\rangle.\end{aligned} \tag{56}$$

To arrive at this expression, we first simplified products of dB_t and $d\Lambda_t$ using the Itō table in Eq. (4). The remaining quantum noise increments satisfy $[dB_t, C_{\mathbf{R}}] = [dB_t^\dagger, C_{\mathbf{R}}] = [d\Lambda_t, C_{\mathbf{R}}] = 0$, since they are defined on non-overlapping time intervals. Thus they can be pulled through $C_{\mathbf{R}}$ and applied directly to the Fock state $|n_\xi\rangle$ via Eq. (13). Finally, the partially projected Fock-states, $|\overline{n}_\xi\rangle = \langle 0_t|n_\xi\rangle$, are the remnants of projecting onto vacuum, see Eq. (20).

To find the unnormalized conditional operators for vacuum detection, we insert Eq. (56) into Eq. (44)

$$\begin{aligned}\bar{\rho}_{m,n}(t+dt|\emptyset) =& \frac{1}{\Pr(\mathbf{R})}\mathrm{Tr}_{\rm field}\Big[C_{\mathbf{R}}\left(\rho_0 \otimes |\overline{m}_\xi\rangle\langle\overline{n}_\xi|\right)C_{\mathbf{R}}^\dagger \\ &- idt\big[H_{\rm sys}, C_{\mathbf{R}}\left(\rho_0 \otimes |\overline{m}_\xi\rangle\langle\overline{n}_\xi|\right)C_{\mathbf{R}}^\dagger\big] \\ &- dt\tfrac{1}{2}\big\{L^\dagger L, C_{\mathbf{R}}\left(\rho_0 \otimes |\overline{m}_\xi\rangle\langle\overline{n}_\xi|\right)C_{\mathbf{R}}^\dagger\big\}_+ \\ &- dt\sqrt{m}\xi(t)L^\dagger S C_{\mathbf{R}}\left(\rho_0 \otimes |\overline{m-1}_\xi\rangle\langle\overline{n}_\xi|\right)C_{\mathbf{R}}^\dagger \\ &- dt\sqrt{n}\xi^*(t)C_{\mathbf{R}}\left(\rho_0 \otimes |\overline{m}_\xi\rangle\langle\overline{n-1}_\xi|\right)C_{\mathbf{R}}^\dagger S^\dagger L\Big].\end{aligned} \tag{57}$$

While the probability of the prior record, $\Pr(\mathbf{R})$, appears, the operators remain unnormalized because the current vacuum-detection probability has not been included.

The critical final step to the derivation lies in writing Eq. (57) exclusively in terms of input Fock states $|n_\xi\rangle$; that is, those defined over the entire input wave-packet mode. This is done by rearrangement of the relative-state decomposition for an n-photon Fock state, given in Eq. (20). Consider the first term in Eq. (57). Under a field trace this relation gives,

$$\begin{aligned}&\mathrm{Tr}_{\rm field}\big[C_{\mathbf{R}}\rho_0 \otimes |\overline{m}_\xi\rangle\langle\overline{n}_\xi|C_{\mathbf{R}}^\dagger\big] \\ &\quad= \mathrm{Tr}_{\rm field}\big[C_{\mathbf{R}}\rho_0 \otimes |m_\xi\rangle\langle n_\xi|C_{\mathbf{R}}^\dagger\big] \qquad (58) \\ &\qquad - dt\sqrt{mn}|\xi(t)|^2\mathrm{Tr}_{\rm field}\big[C_{\mathbf{R}}\rho_0 \otimes |\overline{m-1}_\xi\rangle\langle\overline{n-1}_\xi|C_{\mathbf{R}}^\dagger\big], \\ &\quad= \mathrm{Tr}_{\rm field}\big[C_{\mathbf{R}}\rho_0 \otimes |m_\xi\rangle\langle n_\xi|C_{\mathbf{R}}^\dagger\big] \qquad (59) \\ &\qquad - dt\sqrt{mn}|\xi(t)|^2\mathrm{Tr}_{\rm field}\big[C_{\mathbf{R}}\rho_0 \otimes |m-1_\xi\rangle\langle n-1_\xi|C_{\mathbf{R}}^\dagger\big].\end{aligned}$$

The second term in Eq. (58) is not in terms of the initial wavepacket, so in the second equality we recursively apply the same procedure and keep terms to order dt. Now, we use the definition of $\rho_{m,n}(t)$ in Eq. (40) to get the key relation,

$$\begin{aligned}&\frac{1}{\Pr(\mathbf{R})}\mathrm{Tr}_{\rm field}\big[C_{\mathbf{R}}\rho_0 \otimes |\overline{m}_\xi\rangle\langle\overline{n}_\xi|C_{\mathbf{R}}^\dagger\big] \\ &\qquad = \rho_{m,n}(t) - dt\sqrt{mn}|\xi(t)|^2\rho_{m-1,n-1}(t).\end{aligned} \tag{60}$$

We repeat this procedure for the remaining terms in Eq. (57), neglecting terms of order dt^2. The conditional map in Eq. (57) can now be written entirely in terms of the operators $\rho_{m,n}$,

$$\begin{aligned}\bar{\rho}_{m,n}(t+dt|\emptyset) =& \rho_{m,n} - dt\sqrt{mn}|\xi(t)|^2\rho_{m-1,n-1} \\ &- idt[H, \rho_{m,n}] - dt\tfrac{1}{2}\big\{L^\dagger L, \rho_{m,n}\big\}_+ \\ &- dt\sqrt{m}\xi(t)L^\dagger S\rho_{m-1,n} - dt\sqrt{n}\xi^*(t)\rho_{m,n-1}S^\dagger L.\end{aligned} \tag{61}$$

The operators $\bar{\rho}_{m,n}(t+dt|\emptyset)$ are normalized by the probability of detecting vacuum in the time interval $[t, t+dt)$, *i.e.* $\rho_{m,n}(t+dt|\emptyset) = \bar{\rho}_{m,n}(t+dt|\emptyset)/\Pr(\emptyset)$. To obtain the vacuum-detection probability we substitute the top-level Kraus operators, $\mathcal{M}^N_\emptyset(t)$, into Eq. (47),

$$\begin{aligned}\Pr(\emptyset) =& 1 - \Pr(J) \\ =& 1 - dt\mathrm{Tr}\big[L^\dagger L\rho_{N,N} + \sqrt{N}\xi(t)L^\dagger S\rho_{N-1,N} \\ &+ \sqrt{N}\xi^*(t)\rho_{N,N-1}S^\dagger L + N|\xi(t)|^2\rho_{N-1,N-1}\big].\end{aligned} \tag{62}$$

The probability of vacuum detection is now expressed entirely in terms of the operators $\rho_{m,n}$. The prior normalization, $\Pr(\mathbf{R})^{-1}$, is absorbed into each of the $\rho_{m,n}$ through their definition, Eq. (40). Using the standard Taylor expansion of the denominator to order dt [42] we find

$$\begin{aligned}\rho_{m,n}(t+dt|\emptyset) =& \rho_{m,n} - dt\sqrt{mn}|\xi(t)|^2\rho_{m-1,n-1} \\ &- idt[H, \rho_{m,n}] - dt\tfrac{1}{2}\big\{L^\dagger L, \rho_{m,n}\big\}_+ \\ &- dt\sqrt{m}\xi(t)L^\dagger S\rho_{m-1,n} - dt\sqrt{n}\xi^*(t)\rho_{m,n-1}S^\dagger L \\ &+ \Pr(J)\rho_{m,n}.\end{aligned} \tag{63}$$

The case of photon detection ($R_t = J$) proceeds similarly. The Fock-state Kraus operator for photon detection is

$$\begin{aligned}\mathcal{M}^n_J(t) =&\langle 1_t|U_t C_{\mathbf{R}}|n_\xi\rangle \\ =&\sqrt{dt}\big(LC_{\mathbf{R}}|\overline{n}_\xi\rangle + \sqrt{n}\xi(t)SC_{\mathbf{R}}|\overline{n-1}_\xi\rangle\big). \quad (64)\end{aligned}$$

These are then applied using Eq. (44) to find $\bar{\rho}_{m,n}(t + dt|J)$, just as was done for vacuum detection. Indeed, we follow the same procedure using Eq. (60) to express the right-hand side entirely in terms of the operators $\rho_{m,n}$, to arrive at the expression,

$$\begin{aligned}\bar{\rho}_{m,n}(t+dt|J) =&dtL\rho_{m,n}L^\dagger + dt\sqrt{m}\xi(t)S\rho_{m-1,n}L^\dagger \\ &+ dt\sqrt{n}\xi^*(t)L\rho_{m,n-1}S^\dagger \\ &+ dt\sqrt{mn}|\xi(t)|^2 S\rho_{m-1,n-1}S^\dagger. \quad (65)\end{aligned}$$

The operators $\bar{\rho}_{m,n}(t + dt|J)$ are normalized by dividing by the probability of detecting a photon, $\Pr(J)$, found from Eq. (47) and given explicitly in Eq. (49).

For each infinitesimal measurement outcome $\{\emptyset, J\}$ we have expressed the conditional operators in terms of the $\rho_{m,n}$. Consequently, we may write down a set of coupled differential equations following the usual procedure [8, 43]. For each outcome we use Eq. (46) to get

$$\begin{aligned}d\rho_{m,n}(t|\emptyset) = dt\Big(&- i[H,\rho_{m,n}] - \tfrac{1}{2}\big\{L^\dagger L,\rho_{m,n}\big\}_+ \\ &- \sqrt{m}\xi(t)L^\dagger S\rho_{m-1,n} - \sqrt{n}\xi^*(t)\rho_{m,n-1}S^\dagger L \\ &- \sqrt{mn}|\xi(t)|^2\rho_{m-1,n-1}\Big) + \Pr(J)\rho_{m,n}, \quad (66)\end{aligned}$$

and

$$\begin{aligned}d\rho_{m,n}(t|J) = dt[\Pr(J)]^{-1}\Big(&L\rho_{m,n}L^\dagger \\ &+ \sqrt{m}\xi(t)S\rho_{m-1,n}L^\dagger + \sqrt{n}\xi^*(t)L\rho_{m,n-1}S^\dagger \\ &+ \sqrt{mn}|\xi(t)|^2 S\rho_{m-1,n-1}S^\dagger\Big) - \rho_{m,n}. \quad (67)\end{aligned}$$

The Fock-state SME for photon counting, stated explicitly in Eq. (48), is found by combining the conditional equations for vacuum and photon detection into a single differential equation by introducing a binary random variable dN that satisfies $dN^2 = dN$ and has outcomes 0 (vacuum detection) and 1 (photon detection). The conditional evolution is then concisely expressed as

$$\begin{aligned}d\rho_{m,n}(t) =&dNd\rho_{m,n}(t|J) + (1-dN)d\rho_{m,n}(t|\emptyset). \quad (68)\end{aligned}$$

When a photon is counted ($dN = 1$) the state is updated with Eq. (67), otherwise ($dN = 0$) and it is updated with Eq. (66). Before the current infinitesimal measurement is performed, the conditional expectation value, $\mathbb{E}[dN|\mathbf{R}] = 0 \times \Pr(\emptyset) + 1 \times \Pr(J) = \Pr(J)$, is simply the probability for photon detection. Since $\mathbb{E}[dN|\mathbf{R}]$ is of order dt, terms of order $dNdt$ vanish [21], which gives the Fock-state photon-counting SME in Eq. (48).

An alternate way to write Eq. (48) is in terms of the *photon-counting innovations*, $d\mathcal{J}_C(t) \equiv dN - \mathbb{E}[dN|\mathbf{R}]$, which is Eq. (51). The innovations is the difference between the actual measurement outcome and the expected result and characterizes how much is learned from the measurement. The Fock-state photon-counting SME in Eq. (67) can be transformed to innovations form,

$$\begin{aligned}d\rho_{m,n}(t) = dt\mathcal{L}_{m,n}[\mathbf{G},\xi(t)] + d\mathcal{J}_C(t)d\rho_{m,n}(t|J), \quad (69)\end{aligned}$$

where $\mathcal{L}_{m,n}[\mathbf{G},\xi(t)]$ is defined in Eq. (52).

Provided that one knows the initial system state [44], ensemble averaging over the Fock-state photon-counting SME over trajectories yields the unconditional Fock-state master equations in Ref. [14]. In innovations form this is evident upon inspection since $\mathbb{E}[d\mathcal{J}_C(t)] = 0$ by definition.

C. Fock-state homodyne SME

In homodyne detection, the output field is combined on a balanced beamsplitter with a local oscillator of phase ϕ. The two fields exiting the beamsplitter are sent to photodetectors, whose subtracted photocurrents give the homodyne signal. The conditional evolution under homodyne detection is given by the set of coupled SMEs,

$$\begin{aligned}d\rho_{m,n}(t) = dt\mathcal{L}_{m,n}[\mathbf{G},\xi(t)] + d\mathcal{J}_\phi(t)\mathcal{H}_{m,n}[\mathbf{G},\xi(t),\phi], \quad (70)\end{aligned}$$

where $\mathcal{L}_{m,n}[\mathbf{G},\xi(t)]$, Eq. (52), describes the unconditional evolution, and $\mathcal{H}_{m,n}[\mathbf{G},\xi(t),\phi]$ is a generalization of Wiseman's conditioning map [45],

$$\begin{aligned}\mathcal{H}_{m,n}[\mathbf{G},\xi(t),\phi] \equiv& e^{-i\phi}L\rho_{m,n} + e^{i\phi}\rho_{m,n}L^\dagger \quad (71)\\ &+ e^{-i\phi}\sqrt{m}\xi(t)S\rho_{m-1,n} + e^{i\phi}\sqrt{n}\xi^*(t)\rho_{m,n-1}S^\dagger - K_\phi\rho_{m,n}.\end{aligned}$$

The *expected homodyne current* is given by

$$\begin{aligned}K_\phi =&\mathrm{Tr}\big[(e^{-i\phi}L + e^{i\phi}L^\dagger)\rho_{N,N} \quad (72)\\ &+ e^{-i\phi}\sqrt{N}\xi(t)S\rho_{N-1,N} + e^{i\phi}S^\dagger\sqrt{N}\xi^*(t)\rho_{N,N-1}\big],\end{aligned}$$

which is equivalent to $\mathrm{Tr}[\mathcal{H}_{N,N}[\mathbf{G},\xi(t)]]$. The homodyne innovations $d\mathcal{J}_\phi(t)$,

$$\begin{aligned}d\mathcal{J}_\phi(t) = dJ_\phi - dtK_\phi, \quad (73)\end{aligned}$$

satisfy the properties of a classical Wiener process: zero mean, $\mathbb{E}[d\mathcal{J}_\phi(t)] = 0$, and variance $\mathbb{E}\big[d\mathcal{J}_\phi(t)^2\big] = dt$.

1. *Derivation*

Now that we have a thorough derivation of the Fock-state SME for photon counting, we present the homodyne SME for a quantum system probed by an N-photon Fock state with fewer details, as much of the derivation proceeds in exactly the same way.

The projectors for balanced homodyne measurement in an infinitesimal time interval are constructed from eigenstates of an infinitesimal quadrature operator [39, 43],

$$dQ_\phi = e^{-i\phi}dB_t + e^{i\phi}dB_t^\dagger. \tag{74}$$

The measurement outcomes, labeled by $R_t \in \{\pm\}$, correspond to eigenstates that are equal superpositions,

$$|\pm_t\rangle = \tfrac{1}{\sqrt{2}}\big(|0_t\rangle \pm e^{i\phi}|1_t\rangle\big), \tag{75}$$

with eigenvalues given by $dQ_\phi|\pm_t\rangle = \pm\sqrt{dt}|\pm_t\rangle$ [39, 43]. The associated infinitesimal measurement projectors are

$$\Pi_\pm = I_{t)} \otimes |\pm_t\rangle\langle\pm_t| \otimes I_{[t+dt}. \tag{76}$$

Modeling continuous homodyne measurement as a series of two-outcome measurements is a straightforward consequence of performing infinitesimal measurements in the single-photon sector [39, 43].

The homodyne Kraus operators are obtained from Eq. (45) and Eq. (76). They can be conveniently written as superpositions of the photon-counting Kraus operators, Eq. (56) and Eq. (64):

$$\mathcal{M}^n_\pm(t) = \tfrac{1}{\sqrt{2}}\left[\mathcal{M}^n_\emptyset(t) \pm e^{-i\phi}\mathcal{M}^n_J(t)\right]. \tag{77}$$

The probabilities for the outcomes follow from the Kraus operators [Eq. (47)],

$$\Pr(\pm) = \tfrac{1}{2}\big(1 \pm \sqrt{dt}K_\phi\big), \tag{78}$$

and satisfy $\Pr(+) + \Pr(-) = 1$. We apply the Kraus operators to find the SME for each $\rho_{m,n}$, just as was done for the case of photon counting above. After expanding Eq. (44), we use the relation in Eq. (60) to rewrite the expression entirely in terms of the $\rho_{m,n}$ matrices. Then, the unnormalized conditional operators are

$$\begin{aligned}\bar{\rho}_{m,n}(t+dt|\pm) = \tfrac{1}{2}\big\{&\rho_{m,n} + dt\mathcal{L}_{m,n}[\mathbf{G},\xi(t)] \\ &\pm \sqrt{dt}\big[\mathcal{H}_{m,n}[\mathbf{G},\xi(t),\phi] + K_\phi\rho_{m,n}\big]\big\},\end{aligned} \tag{79}$$

where the homodyne conditioning map $\mathcal{H}_{m,n}[\mathbf{G},\xi(t),\phi]$ and expected homodyne current K_ϕ are given in Eqs. (71-72).

The conditional states, Eq. (79), and probabilities, Eq. (78), are combined into differential equations for each $\rho_{m,n}$ using Eq. (46) by expanding the denominator to order dt and collecting terms. We introduce a random variable dJ_ϕ that takes on values $\pm\sqrt{dt}$. From the conditional expectation values $\mathbb{E}[dJ_\phi|\mathbf{R}] = \sqrt{dt}\times\Pr(+) - \sqrt{dt}\times\Pr(-) = dtK_\phi$ and $\mathbb{E}[dJ_\phi^2|\mathbf{R}] = dt$, the variance of dJ_ϕ is dt. Thus we define the *homodyne innovations* as $d\mathcal{J}_\phi(t) \equiv dJ_\phi - \mathbb{E}[dJ_\phi|\mathbf{R}]$ which is equivalent to Eq. (73). As stated above, this satisfies the properties of a classical Wiener process: mean zero and variance dt. After some algebra, the differential updates corresponding to each measurement are combined into the Fock-state homodyne SME, Eq. (70).

D. Fock-state heterodyne SME

Continuous heterodyne detection [8, 43, 46–48] simultaneously measures two orthogonal quadratures, either by mixing the output fields with a detuned local oscillator or performing double homodyne detection. For orthogonal quadratures specified by the phases $\phi \in \{0, \pi/2\}$, the Fock-state heterodyne SME is

$$\begin{aligned}d\rho_{m,n}(t) =& dt\mathcal{L}_{m,n}[\mathbf{G},\xi(t)] \\ &+ \tfrac{1}{\sqrt{2}}d\mathcal{J}_0(t)\mathcal{H}_{m,n}[\mathbf{G},\xi(t),0] \\ &+ \tfrac{1}{\sqrt{2}}d\mathcal{J}_{\pi/2}(t)\mathcal{H}_{m,n}[\mathbf{G},\xi(t),\pi/2],\end{aligned} \tag{80}$$

where $\mathcal{L}_{m,n}[\mathbf{G},\xi(t)]$, Eq. (52), describes the unconditional evolution, and $\mathcal{H}_{m,n}[\mathbf{G},\xi(t),\phi]$ is the conditioning map for each quadrature, Eq. (71). Each quadrature has a homodyne innovations $\mathcal{J}_\phi(t)$, Eq. (73), satisfying the properties of a classical Wiener process.

1. *Derivation*

As measurements of orthogonal quadratures do not commute, heterodyne detection is a more general measurement of the field described by a positive-operator valued measure (POVM).

In an infinitesimal time interval each quadrature is described by Eq. (74) with phases $\phi \in \{0, \pi/2\}$, respectively. Each quadrature measurement has two outcomes, which are not independent, giving the four joint outcomes $\{+\widetilde{+}, +\widetilde{-}, -\widetilde{+}, -\widetilde{-}\}$. The Kraus operators of the infinitesimal field measurement are

$$\Upsilon_{\pm,\widetilde{\pm}} = I_{t)} \otimes \frac{|\pm,\widetilde{\pm}_t\rangle\langle\pm,\widetilde{\pm}_t|}{\sqrt{2}} \otimes I_{[t+dt}, \tag{81}$$

which are composed of the four nonorthogonal states,

$$|\pm,\widetilde{\pm}_t\rangle = \frac{1}{\sqrt{2}}\left(|0_t\rangle + \frac{\pm 1\widetilde{\pm}i}{\sqrt{2}}|1_t\rangle\right). \tag{82}$$

The POVM elements corresponding to the outcomes are $E_{\pm,\widetilde{\pm}} = \Upsilon^\dagger_{\pm,\widetilde{\pm}}\Upsilon_{\pm,\widetilde{\pm}} = \frac{1}{2}|\pm,\widetilde{\pm}_t\rangle\langle\pm,\widetilde{\pm}_t|$ and obey $\sum_{s,r} E_{s,r} = I_t$.

The heterodyne Kraus oprators can be written in terms of the photon-counting Kraus operators, Eq. (56) and Eq. (64),

$$\mathcal{M}^n_{\pm,\widetilde{\pm}}(t) = \frac{1}{2}\left[\mathcal{M}^n_\emptyset(t) + \tfrac{1}{\sqrt{2}}(\pm 1\widetilde{\pm}i)\mathcal{M}^n_J(t)\right]. \tag{83}$$

The outcomes probabilities follow from Eq. (47),

$$\Pr(\pm,\widetilde{\pm}) = \frac{1}{4}\left[1 + \sqrt{\tfrac{dt}{2}}\big(\pm K_0\widetilde{\pm}K_{\pi/2}\big)\right] \tag{84}$$

where K_ϕ are the quadrature currents, Eq. (72).

For each measured quadrature we define a random variable, $dJ_0 = \pm\sqrt{dt}$ and $dJ_{\pi/2} = \widetilde{\pm}\sqrt{dt}$, that satisfy the

property $dJ_i dJ_j = dt\delta_{i,j}$ so that $[(dJ_i + dJ_j)/\sqrt{2}]^2 = dt$. The statistics are found from the marginal probability distributions, e.g. $\Pr(\widetilde{\pm}) = \Pr(-, \widetilde{\pm}) + \Pr(+, \widetilde{\pm})$, and for each we define an innovations akin to Eq. (73). Following the same procedure in Sec. III C, we obtain Eq. (80).

E. Conditional expectation values

The conditional expectation value of a joint operator $\mathcal{O} \in \mathcal{H}_{\rm sys} \otimes \mathcal{H}_{\rm field}$ is

$$\mathbb{E}[\mathcal{O}(t)|\mathbf{R}] \equiv \frac{1}{\Pr(\mathbf{R})} \mathrm{Tr}\big[C_{\mathbf{R}} \rho_0 \otimes |N_\xi\rangle\langle N_\xi| C_{\mathbf{R}}^\dagger \mathcal{O}\big]. \quad (85)$$

For system operators, $\mathcal{O} = X(t_0) = X \otimes I_{\rm field}$, performing the field trace allows the conditional expectation value to be written in terms of the reduced system state that arises from the solutions of the SMEs above,

$$\mathbb{E}[X(t)|\mathbf{R}] = \mathrm{Tr}[\rho_{\rm sys}(t) X]. \quad (86)$$

Conditional expectation values for general field operators do not have as simple a reduction as in Eq. (86). However, for the output quantum noise increments given by Eq. (6), $\mathcal{O} = I_{\rm sys} \otimes dB_t^{\rm out}$ and $\mathcal{O} = I_{\rm sys} \otimes d\Lambda_t^{\rm out}$, the conditional expectation values are readily calculated for Fock-state input. Using the solutions to the Fock-state SMEs, conditional expectation values of field observables can be calculated. Inserting the Hermitian output field observables, $d\Lambda_t^{\rm out}$ and $dQ_\phi^{\rm out}$, into Eq. (85),

$$\mathbb{E}[d\Lambda_t^{\rm out}|\mathbf{R}] = \Pr(J), \quad (87a)$$
$$\mathbb{E}[dQ_\phi^{\rm out}|\mathbf{R}] = dt K_\phi. \quad (87b)$$

These quantities have indeed already appeared in the probabilities for the measurement outcomes, Eq. (49) and Eq. (78). The conditional statistics for infinitesimal measurements are fully determined by four operators: the reduced system state $\rho_{N,N}$ along with the three auxiliary operators, $\rho_{N-1,N}$, $\rho_{N,N-1}$, and $\rho_{N-1,N-1}$. This is a straightforward consequence of the fact that such measurements are described in a basis with at most one photon.

As an example, we may be interested in the conditional photon counting statistics given homodyne measurements up to time t. We first solve Eq. (70) for a given homodyne record $\mathbf{R}$, then use the solutions to calculate $\Pr(J)$, which is equivalent to $\mathbb{E}[d\Lambda_t^{\rm out}|\mathbf{R}]$ according to Eq. (87a).

F. System-field entanglement

As the quantum system and input Fock state interact they become entangled, and at intermediate times signatures of this entanglement are present in the reduced system state. Although the measurements disentangle the portion of the field that has been detected, entanglement between the quantum system and future field persists.

Indeed, even when the input system state is pure, a trace over the field yields a *mixed* reduced state since the system has become correlated with the unmeasured field, as was studied recently for a two-level atom interacting with a single-photon Fock state [49]. This is in contrast to input field states that factorize temporally, where the reduced conditional state remains pure if the field is measured with perfect efficiency. Thus, a stochastic Schrödinger equation for a pure-state wavefunction does not apply for Fock-state input, and one is required to use SMEs.

IV. GENERALIZATIONS

A. Superpositions and mixtures of Fock states in the same wave packet

In this section, we generalize the Fock-state SMEs to input states that are superpositions and mixtures of Fock states. Since the Fock states, $|n_\xi\rangle$, form a complete basis in the temporal mode $\xi(t)$, they can be used to construct any state in that wave packet. For an initial field state

$$\rho_{\rm field}(t_0) = \sum_{m,n} c_{m,n} |m_\xi\rangle\langle n_\xi|, \quad (88)$$

there are two modifications to the Fock-state SMEs presented in Sec. III. First, the reduced system state is constructed from the $\rho_{m,n}(t)$ using the coefficients $c_{m,n}$. Second, this reduced system state changes the form of the measurement probabilities. However, the coupled SMEs are *identical* to those for pure Fock-state input. Below we discuss the details.

Given an input field with the form of Eq. (88), the reduced system state at time t is

$$\rho_{\rm sys}(t) = \sum_{m,n} c_{m,n} \rho_{m,n}(t), \quad (89)$$

where $\rho_{m,n}(t)$ are solutions to the respective Fock-state SMEs in Sec. III (photon counting, homodyne, or heterodyne). That is, the form of the SMEs that couple the $\rho_{m,n}$ operators is not modified for different input field states. However, the diagonal elements and off-diagonal coherences in Eq. (88) do affect measurements of the output fields by modifying the conditional probabilities, $\Pr(R_t)$, that normalize the post-measurement matrices $\rho_{m,n}(t)$.

For the Fock-state photon-counting SME the probability of detecting a photon at time t becomes

$$\begin{aligned}\Pr(J) =& dt \sum_{m,n} c_{m,n} \mathrm{Tr}\big[L^\dagger L \rho_{m,n} + \sqrt{m}\xi(t) L^\dagger S \rho_{m-1,n} \\ &+ \sqrt{n}\xi^*(t) S^\dagger L \rho_{m,n-1} + \sqrt{mn}|\xi(t)|^2 \rho_{m-1,n-1}\big],\end{aligned} \quad (90)$$

with the probability of vacuum detection given by $\Pr(\emptyset) = 1 - \Pr(J)$. The photon-counting SME for superpositions/mixtures of Fock states is found by using the detection probability, Eq. (90), in either form of the Fock-state photon-counting SME, Eq. (48) and Eq. (69). The reduced system state is found by combining the solutions according to Eq. (89).

For homodyne detection the probabilities $\Pr(\pm)$ and conditioning map $\mathcal{H}_{m,n}[\mathbf{G}, \xi(t), \phi]$, Eq. (78) and Eq. (71), involve the modified expected quadrature current,

$$K_\phi = \sum_{m,n} c_{mn} \mathrm{Tr}\big[(e^{-i\phi}L + e^{i\phi}L^\dagger)\rho_{m,n} + e^{-i\phi}\sqrt{m}\xi(t)S\rho_{m-1,n} + e^{i\phi}\sqrt{n}\xi^*(t)S^\dagger\rho_{m,n-1}\big]. \tag{91}$$

The homodyne SME for superposition/mixtures of Fock states is found by using the modified K_ϕ, Eq. (91), in the Fock-state homodyne SME, Eq. (70), and then combining the solutions according to Eq. (89) to get the reduced system state. The Fock-state heterodyne SME, Eq. (80), is modified similarly.

In Appendix B we give the Heisenberg-picture form of the Fock-state SMEs for the general input fields in Eq. (88).

B. Imperfect detection

To model detectors of imperfect quantum efficiency η ($0 \le \eta \le 1$) the Fock-state SMEs and unconditional Fock-state master equations are combined with respective weights η and $1-\eta$ [8]. For photon counting, the standard-form Fock-state photon-counting SME becomes

$$d\rho_{m,n}(t) = dN_\eta d\rho_{m,n}(t|J) + \eta d\rho_{m,n}(t|\emptyset) + dt(1-\eta)\mathcal{D}_L[\rho_{m,n}]. \tag{92}$$

The probability $\Pr(J)$ is a statement about the *output field*—it is the probability that a photon arrives at the detector. However, the fact that an imperfect detector may not register the photon is captured by the modified conditional expectation value, $\mathbb{E}[dN_\eta|\mathbf{R}] = \eta \Pr(J)$. Inserting this relation in the photon-counting innovations, Eq. (51), the transformation to the innovations-form SME is straightforward. For homodyne and heterodyne detection, the Fock-state SMEs are obtained by modifying the innovations in Eqs. (70) and (80) according to $d\mathcal{J}_\phi(t) \to \sqrt{\eta}d\mathcal{J}_\phi(t)$ [8].

C. Additional decoherence

Additional decoherence channels can be included by amending the Fock-state SMEs. For each $\rho_{m,n}$ the actions of the Lindblad superoperators corresponding to the decoherence channels are added to the differential maps $d\rho_{m,n}(t)$. When the dissipation arises from heat baths, it can be derived explicitly by including additional modes in the evolution unitary, Eq. (5), and then tracing them out. For example, a stationary thermal bath with mean photon number $\langle n\rangle$ that couples linearly to the system via the operators $\tilde{L}$ and $\tilde{L}^\dagger$ introduces additional Lindblad terms the equations of motion for $\rho_{m,n}(t)$. Specifically, to each $d\rho_{m,n}(t)$ the following terms are added,

$$\sqrt{\langle n\rangle + 1}\mathcal{D}_{\tilde{L}}[\rho_{m,n}] + \sqrt{\langle n\rangle}\mathcal{D}_{\tilde{L}^\dagger}[\rho_{m,n}], \tag{93}$$

where the first describes decay and the second incoherent thermal driving.

V. EXAMPLE: CONDITIONAL DYNAMICS OF A TWO-LEVEL ATOM

As an introduction and guide to using the Fock-state SMEs, we present a brief study of conditional dynamics for a two-level atom with eigenstates $|g\rangle$ and $|e\rangle$. The total Hamiltonian ($\hbar = 1$) for the atom-field system is

$$H = H_{\mathrm{atom}} + H_{\mathrm{field}} + H_{\mathrm{int}}. \tag{94}$$

The bare Hamiltonian for the atom with transition frequency ω_0 is $H_{\mathrm{atom}} = \frac{\omega_0}{2}\sigma_z$, where $\sigma_z = |e\rangle\langle e| - |g\rangle\langle g|$. The positive-frequency, continuous-mode field is described by a bare Hamiltonian $H_{\mathrm{field}} = \int_0^\infty d\omega\, \omega b^\dagger(\omega)b(\omega)$, with field operators satisfying $[b(\omega), b^\dagger(\omega')] = \delta(\omega - \omega')$. Finally, the atom-field interaction is described by the Hamiltonian [21],

$$H_{\mathrm{int}} = -i\int_0^\infty d\omega\, \kappa(\omega)\big[\sigma_+ b(\omega) - \sigma_- b^\dagger(\omega)\big], \tag{95}$$

where $\kappa(\omega)$ is the dipole-field interaction strength at frequency ω, and $\sigma_+ = |e\rangle\langle g|$ and $\sigma_- = |g\rangle\langle e|$ are the atomic raising and lowering operators. Making the usual Markov approximation [5, 21], the coupling strength is linearized around the atomic resonance frequency, $\Gamma \equiv 2\pi|\kappa(\omega_0)|^2$ and the lower limit of integration in Eq. (95) is extended to $-\infty$. In an interaction picture with respect to $H_0 = \frac{\omega_c}{2}\sigma_z + H_{\mathrm{field}}$, where ω_c is the carrier frequency of the input wave packet, the resulting (S, L, H)-operators that appear in the time evolution operator, Eq. (5), are

$$S = I_{\mathrm{sys}}, \tag{96a}$$
$$L = \sqrt{\Gamma}\sigma_-, \tag{96b}$$
$$H_{\mathrm{sys}} = -\Delta_0\sigma_z, \tag{96c}$$

with $\sigma_z = |e\rangle\langle e| - |g\rangle\langle g|$ and detuning $\Delta_0 \equiv \omega_c - \omega_0$. The atom is probed by a Fock state $|N_\xi\rangle$ [Eq. (12)] with resonant carrier frequency ($\omega_c = \omega_0$) in a Gaussian wave packet given by

$$\xi(t) = \left[\frac{(\Delta_\omega/\Gamma)^2}{2\pi}\right]^{1/4} \exp\left[-\frac{(\Delta_\omega/\Gamma)^2}{4}(t-t_0)^2\right]. \tag{97}$$

The dimensionless spectral bandwidth, Δ_ω/Γ, is defined such that the variance of $|\xi(t)|^2$ is $(\Delta_\omega/\Gamma)^{-2}$.

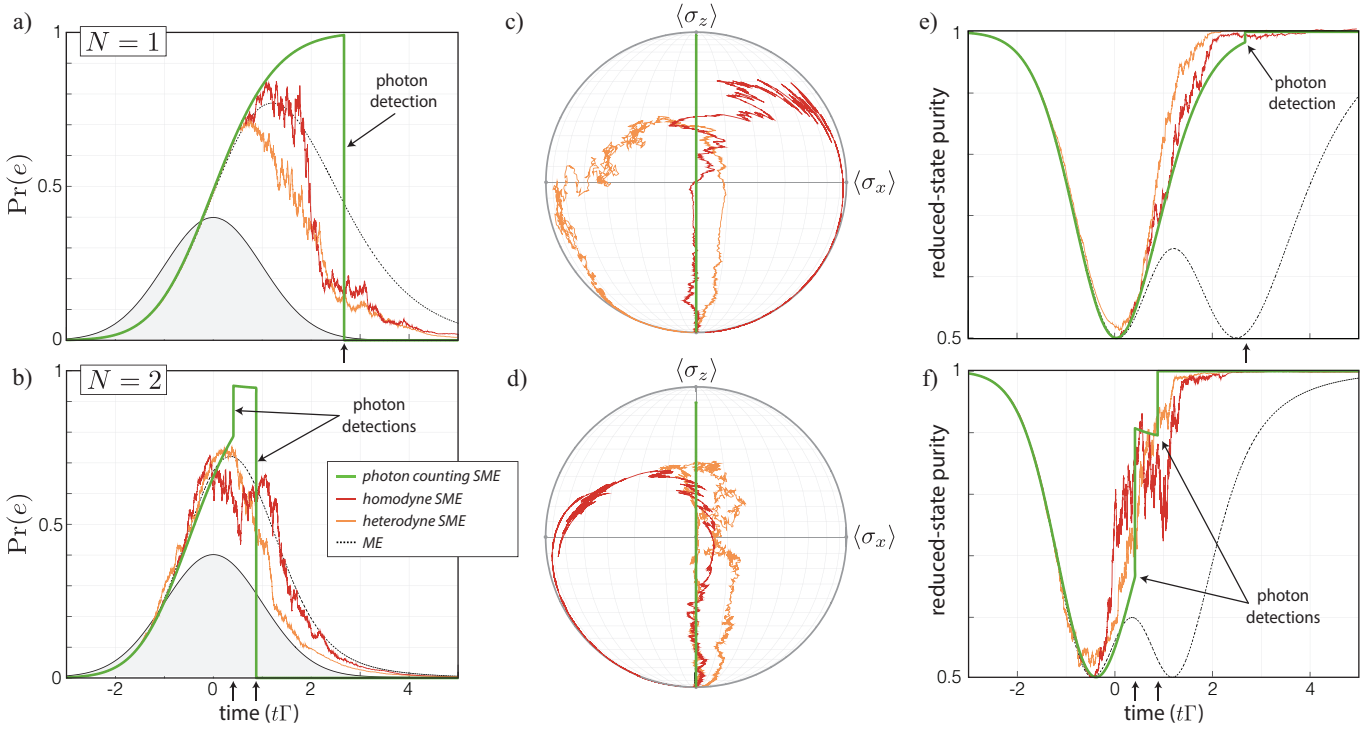

FIG. 2. Single trajectories for a two-level atom interacting with propagating $N = 1$ (top row) and $N = 2$ (bottom row) Fock states when the output fields are subject to continuous photon counting, homodyne, and heterodyne measurements. Detection times are indicated for the photon-counting trajectory. Unconditional dynamics, calculated from the Fock-state master equation, are shown. (a–b) Conditional excitation probability $\Pr(e) = \langle e|\rho_{\rm sys}(t)|e\rangle$. The input Gaussian wave packet $|\xi(t)|^2$ is shown (thin black filled grey), where $\xi(t)$ is given by Eq. (97) with $\Delta_\omega/\Gamma = 1$ and $t_0 = 0$. (c–d) Projection of the Bloch sphere onto the xz-plane showing the trajectories of the conditional Bloch vector. (e–f) Conditional reduced-state purity, $\mathrm{Tr}[\rho^2_{\rm sys}(t)]$, for the same trajectories.

A. Few-photon Fock states

We solve the Fock-state SMEs in Section III for few-photon input for each of the three measurements: photon counting, homodyne, and heterodyne. For each measurement type we calculate a single trajectory for the atom initialized in its ground state, $\rho_0 = |g\rangle\langle g|$, and the input field in an N-photon Fock state. We numerically integrate the set of coupled equations for $\rho_{m,n}$ and then extract the conditional reduced system state: $\rho_{\rm sys} = \rho_{N,N}$. From $\rho_{\rm sys}$, conditional expectation values are then calculated as usual, see Eq. (86).

1. *Single quantum trajectories*

We begin by examining the conditional excitation probability, Eq. (86), for $\Pr(e) \equiv \mathrm{Tr}[|e\rangle\langle e|\rho_{\rm sys}(t)]$ for each of the measurement types. In Fig. 2 we plot single trajectories for $N = 1$ and $N = 2$ input photons. The trajectories for photon counting are of particular interest, as Fock states are eigenstates of total photon number. These trajectories display discrete jumps at the photon detection times—in (a) there is one jump, and in (b) there are two, corresponding to the number of input photons N. The vacuum-detection evolution up to the first detection time is deterministic, given by the first line of Eq. (48). At the first detection time the single-photon trajectory returns to zero, indicating a quantum jump to the atom's ground state.

However, something curious happens for the $N = 2$ trajectory in Fig. 2(b): $\Pr(e)$ abruptly increases at the first photon detection. Similar quantum jumps up have recently been studied by Blocher and Mølmer [50] for a decaying atom. Indeed, the conditional excitation probability may jump up or down depending on time of detection (see Fig. 2(c)). Further simulations (not shown) indicate that this is a generic feature of photon counting arising from interference between input and reradiated fields.

Insight into the conditional dynamics can be seen in the trajectories of the Bloch vector, $\vec{\sigma} = (\langle\sigma_x\rangle, \langle\sigma_y\rangle, \langle\sigma_z\rangle)$, shown in Fig. 2(c-d). The Bloch-vector components are $\langle\sigma_i(t)\rangle \equiv \mathrm{Tr}[\rho_{\rm sys}(t)\sigma_i]$ for Pauli operators on the pseudospin, $\sigma_x = |e\rangle\langle g| + |g\rangle\langle e|, \sigma_y = -i(|e\rangle\langle g| - |g\rangle\langle e|)$. As pure Fock states have no associated phase, the excitation dynamics for photon counting trajectories lie entirely on the z-axis of the Bloch sphere. At the center of the Bloch sphere, where $\Pr(e) = 0.5$, the atom is maximally entangled with the field and the

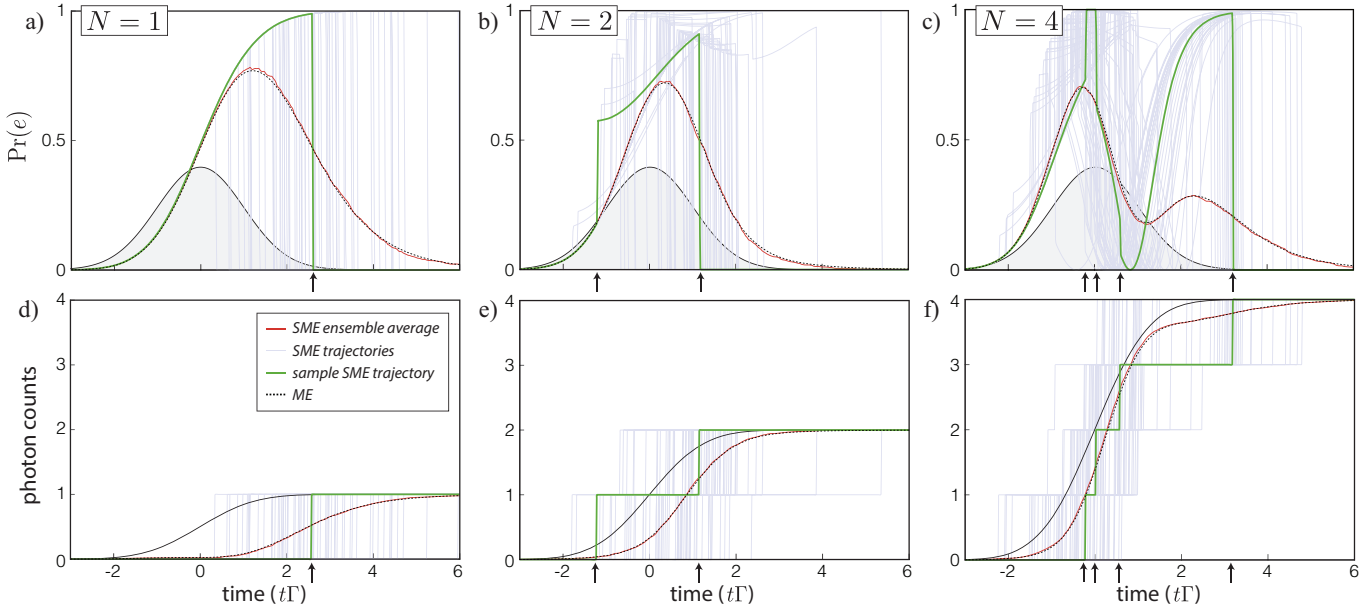

FIG. 3. Ensemble-averaged expectation values for a two-level interacting with Fock states with $N = 1$ (left column), $N = 2$ (middle column) $N = 4$ (right column) photons for continuous photon counting measurements. 1000 trajectories were simulated, 60 of which are shown. A single example trajectory is highlighted (solid curve exhibiting jumps) with times of detection indicated by black arrows on the time axis. The ensemble average over trajectories converges to the unconditional Fock-state master equation. (a–c) Excitation probability $\Pr(e)$. The input Gaussian wave packet $|\xi(t)|^2$ is shown (thin black filled grey), where $\xi(t)$ is given by Eq. (97) with $\Delta_\omega/\Gamma = 1$ and $t_0 = 0$. (d–f) Total photon counts as a function of time. Every trajectory has exactly N photon counts, and the asymptotic ensemble averages and unconditional expectation values approach N. Average total photon counts for the input Gaussian wave packet, $\int_0^t dt N|\xi(t)|^2$, is shown in black.

reduced state reaches its minimum purity. For the diffusive cases of homodyne and heterodyne detection, the phases associated with the measurements drive the reduced atomic state off the z-axis, as seen in the Bloch-sphere representations of the state in Fig. 2(a-b). This results in reduced states of higher purity in general. Since the atom is prepared in a pure state, atom-field entanglement is revealed by the reduced-state purity of the atom, $\mathrm{Tr}[\rho^2_{\mathrm{sys}}(t)]$, plotted in Fig. 2(e-f).

2. *Ensemble-averaged quantities*

In early work by Dalibard *et al.* [51], quantum trajectories for vacuum input fields were used not as a description of a single-shot continuous measurement, but rather as a tool to efficiently simulate ensemble-averaged, unconditional evolution. This relies on the fact that as the number of trajectories becomes large, the ensemble average over quantum trajectories approaches the unconditional master equation (ME). Convergence to the ME is similarly true for Fock-state input fields, as demonstrated in Fig. 3. For each input field preparation with $N = \{1, 2, 4\}$ photons, we simulated 1000 trajectories of the photon-counting SMEs. In the top row, we illustrate agreement of the ensemble-averaged SME and the ME for $\Pr(e)$.

Below, in the second row of Fig. 3, we plot total photon counts as a function of time. In any particular trajectory the photon detection times are random, but as $t \to \infty$ the total number of detections is equal to the number of input photons. The ensemble average over trajectories approaches the unconditional integrated photon flux, $\int_0^t \langle d\Lambda_{t'}\rangle$. This is directly calculated from the input-output field relation, Eq. (7), using the Fock-state MEs as described in Ref. [14].

B. Fock-state approximation to a coherent state

A continuous-mode coherent state with amplitude $\alpha(t) = \alpha_0\xi(t)$, with peak amplitude α_0 [52], can be expanded in the basis of Fock states as [35]

$$|\alpha_\xi\rangle = e^{-|\alpha_0|^2/2}\sum_{n=0}^{\infty}\frac{(\alpha_0)^n}{\sqrt{n!}}|n_\xi\rangle. \tag{98}$$

The total mean photon number is $\langle n\rangle = |\alpha_0|^2$ and peak input photon flux is $\langle n\rangle \max|\xi(t)|^2$. A finite approximation to $|\alpha_\xi\rangle$ is found by truncating the Fock expansion at chosen photon number n_{trunc}.

We return to the two-level atom in Sec. V. Here, we consider the case where the atom is probed by a coherent-state wave packet $|\alpha_\xi\rangle$ with amplitude $\alpha_0 = \sqrt{5}$ corresponding to $\langle n\rangle = 5$, and the output fields are measured via continuous homodyne detection. The wave packet is

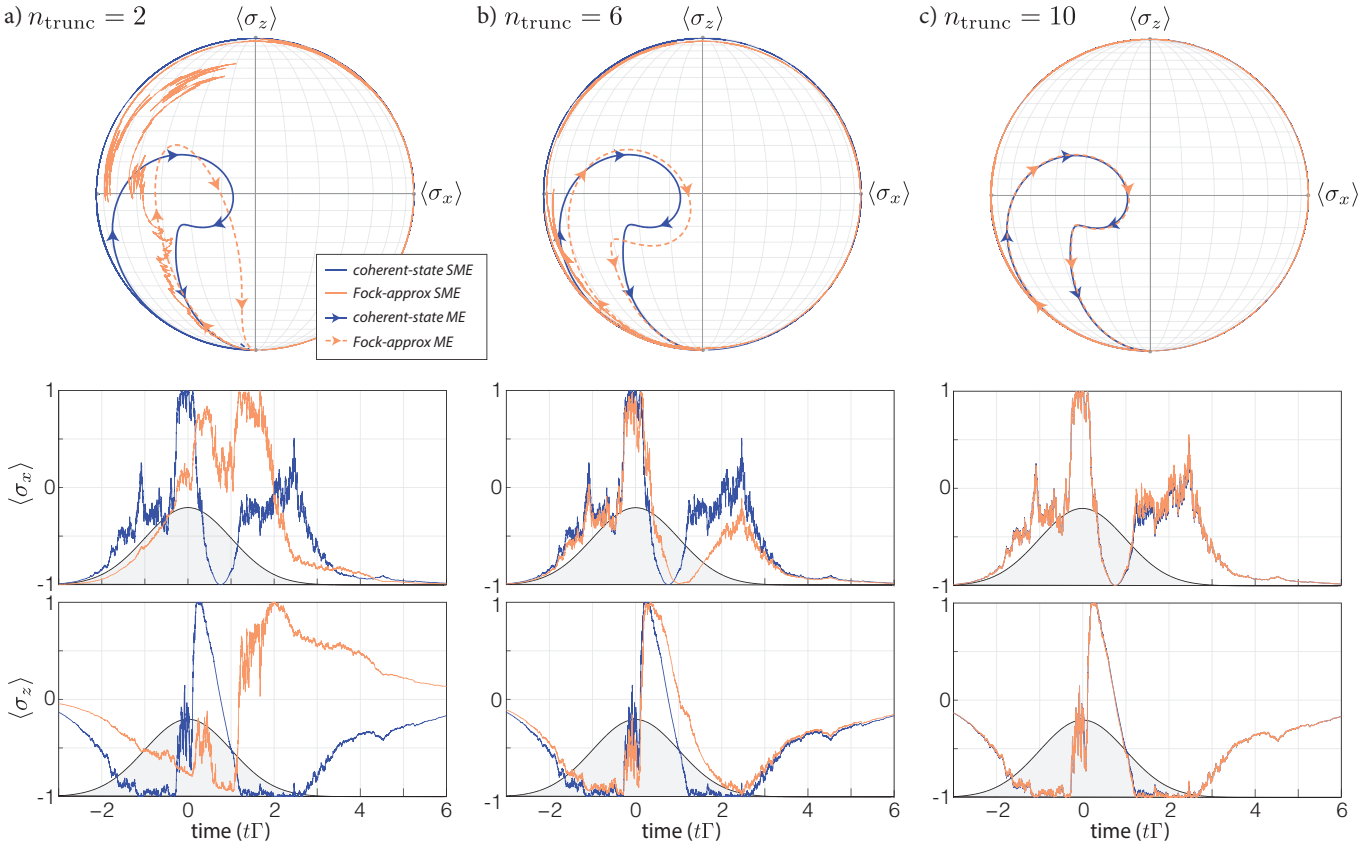

FIG. 4. Trajectories for a two-level atom interacting with finite approximations (red) to a coherent-state wave packet (blue) of increasing precision (Fock-state truncation level $n_{\rm trunc}$), when the output fields are subject to homodyne detection. The coherent state is prepared with $\langle n\rangle = 5$ photons. Convergence of a single trajectory is shown under the same noise realization (simulated measurement record). (a-c) Projection of the Bloch sphere onto the xz-plane showing the trajectories of the conditional Bloch vectors with respective Fock-state approximations. The approximations are truncated at $n_{\rm trunc} = \{2, 6, 10\}$, which account for $\{0.04, 0.62, 0.97\}$ of the total photons in the coherent state. For comparison, the Bloch vectors for the coherent-state and Fock-state-approximation master equations are shown. Below each Bloch sphere are the dynamics of $\langle\sigma_x(t)\rangle$ and $\langle\sigma_z(t)\rangle$. For reference the input Gaussian wave packet $|\xi(t)|^2$ is shown in black filled grey, where $\xi(t)$ is given by Eq. (97) with $\Delta_\omega/\Gamma = 1$ and $t_0 = 0$.

Gaussian, Eq. (97), with $\Delta_\omega/\Gamma = 1$. In Fig. 4 we compare the conditional coherent-state dynamics to those for Fock-state approximations of increasing truncation $n_{\rm trunc}$ in Eq. (98). The input state is a superposition of Fock states, so the reduced system state is given by Eq. (89). Under identical measurement records, the approximate Fock-state conditional expectation values converge to the coherent-state values as the truncation level increases, as seen in columns (a–c). Shown for comparison are the unconditional ME dynamics for the Fock-state approximation [14, 53], which likewise converges.

For coherent-state input, the conditional state of the atom remains pure at all times and its Bloch vector is confined to the surface of the Bloch sphere. Any entanglement generated between the atom and field is immediately recovered by the continuous measurements, which project the joint state into a tensor-product state. This is evident from the coherent-state trajectory, which traces out the boundary of the Bloch sphere in the xz-plane. When the truncation level of the the Fock-state approximations is low, Fig 4(a) for example, the conditional Bloch vector enters the interior and the reduced-state becomes mixed, signaling residual entanglement with the future, unmeasured field.

VI. CONCLUSION

We have presented the stochastic master equations that describe the conditional reduced-state dynamics for a quantum system interacting with a propagating N-photon Fock state. Our derivation of the Fock-state SMEs for different detection schemes uses Kraus operators and a temporal decomposition of the input fields, rather than the methods of quantum filtering theory [34].

A method complementary to our coupled SMEs exists, which treats the input Fock state as arising from a cascaded source. This was originally suggested for a single

photon by Gheri *et al.* [13] and Gough *et al.* [17, 18], and generalized to N photons by Gough and Zhang [54]. Further, many alternative approaches have been developed to study quantum interactions with propagating photons. These include path-integral-based master equations [55], generalized input-output theory [56], direct calculations of the scattering matrix [57], time-domain treatment of the joint-state wavefunction [58–60], and diagrammatic methods [61]. It would be interesting to see if such methods could be extended to describe field measurements and the resulting quantum trajectories.

The Fock-state SMEs presented here can be extended to more general fields. For input states with large mean fields, a Mollow transformation can be used to reduce the number of Fock states required for a faithful simulation [31, see Sec. VII B 1]. By choosing a temporal-mode basis, as was done for Fock-state MEs in Refs. [14, 53], our methods can be straightforwardly extended to more general N-photon states whose spectral density functions do not factorize [62]. Recently, using a non-Markovian embedding in the Heisenberg picture, SMEs for such states were derived by Song *et al.* in Ref. [19].

There are a number of applications of our theory. Single-photon SMEs have already been used to study conditional phase shifts on a cavity [63], nondestructive photon detection [64], and conditional excitation probabilities [18, 65]. Two-mode, two-photon quantum trajectories have been used to study an effective beamsplitter interaction using a mechanical resonator [66] and excitation probabilities [67]. It is forseeable that our formalism could enable the study of high-speed quantum feedback control [8, 68] with nonclassical fields. Further, the Fock-state SMEs could allow for novel state preparation using time-resolved post-selection, where the number of photons detected as well as the *times of detection* are design parameters. Finally, the techniques of Sec. IV A allow for the direct simulation of SMEs for exotic field states by expressing them in a Fock basis.

Another broad application of the Fock-state SMEs is the study of quantum networks with nonclassical inputs. Carmichael and Gardiner [15, 16] developed the theory of *cascaded quantum systems* for situations where one quantum system is driven by the output of another. Recently, this theory was expanded to include the scattering operator S and formalized into the *SLH framework* for quantum networks [69]. For a set of n cascaded quantum systems, the theory describes rules to compose the separate Hamiltonians $H^{(n)}$, linear coupling operators $L^{(n)}$, and scattering operators $S^{(n)}$ for into a set of new $(S, L, H)_{\text{cas}}$ operators that describes the joint system as a whole. An introduction can be found in Ref. [31]. The cascaded coupling operators, $(S, L, H)_{\text{cas}}$, are used directly in the Fock-state SMEs above. Using the results in Sec. IV A, our formalism allows simulating an arbitrary field state input to the network.

Acknowledgements: The authors would like to thank (in alphabetical order): Sahar Basiri-Esfahani, Agata Brańczyk, Carl Caves, Robert Cook, Ivan Deutsch, Bixuan Fan, Julio Gea-Banacloche, John Gough, Michael Jack, Matthew James, Zhang Jiang, Göran Johansson, Anton Kockum, Casey Myers, Gerard Milburn, Hendra Nurdin, Nicolas Quesada, Sankar Sathyamoorthy, Tom Stace, Lars Tornberg, and Howard Wiseman for discussions on related topics over the last several years. BQB thanks the Perimeter Institute for financial support during several research visits. This research was supported in part by the ARC Centre of Excellence in Engineered Quantum Systems (EQuS), Project No. CE110001013. BQB and JC acknowledge financial support from NSF Grant No. PHY-0969997, No. PHY-0903953, No. PHY-1005540, and No. PHY-1521016, ONR Grant No. N00014-11-1-008, and AFOSR Grant No. Y600242. JC was supported by the Australian Research Council via DE160100356 and the Perimeter Institute for Theoretical Physics. Research at Perimeter Institute is supported by the Government of Canada through the Department of Innovation, Science and Economic Development Canada and by the Province of Ontario through the Ministry of Research, Innovation and Science.

[1] A. Reiserer and G. Rempe, "Cavity-based quantum networks with single atoms and optical photons," Rev. Mod. Phys. **87**, 1379 (2015).
[2] M. Hofheinz, E. M. Weig, M. Ansmann, R. C. Bialczak, E. Lucero, M. Neeley, A. D. O'Connell, H. Wang, J. M. Martinis, and A. N. Cleland, "Generation of fock states in a superconducting quantum circuit," Nature **454**, 310 (2008).
[3] B. Peaudecerf, C. Sayrin, X. Zhou, T. Rybarczyk, S. Gleyzes, I. Dotsenko, J. M. Raimond, M. Brune, and S. Haroche, "Quantum feedback experiments stabilizing fock states of light in a cavity," Phys. Rev. A **87**, 042320 (2013).
[4] M. Cooper, L. J. Wright, C. Söller, and B. J. Smith, "Experimental generation of multi-photon fock states," Opt. Express **21**, 5309 (2013).
[5] H. J. Carmichael, *An Open Systems Approach to Quantum Optics*, Lecture Notes in Physics Monographs, Vol. 18 (Springer-Verlag Berlin Heidelberg, 1993) lectures Presented at the Université Libre de Bruxelles, October 28 to November 4, 1991.
[6] H. J. Carmichael, *Statistical Methods in Quantum Optics 2: Non-Classical Fields*, Theoretical and Mathematical Physics (Springer-Verlag Berlin Heidelberg, 2008).
[7] H. M. Wiseman, *Quantum trajectories and feedback*, Ph.D. thesis, University of Queensland (1994).
[8] H. M. Wiseman and G. J. Milburn, *Quantum Measurement and Control* (Cambridge University Press, 2010).

[9] K. W. Murch, S. J. Weber, C. Macklin, and I. Siddiqi, "Observing single quantum trajectories of a superconducting quantum bit," Nature **502**, 211 (2013).

[10] P. Campagne-Ibarcq, P. Six, L. Bretheau, A. Sarlette, M. Mirrahimi, P. Rouchon, and B. Huard, "Observing quantum state diffusion by heterodyne detection of fluorescence," Phys. Rev. X **6**, 011002 (2016).

[11] A. Chantasri, M. E. Kimchi-Schwartz, N. Roch, I. Siddiqi, and A. N. Jordan, "Quantum trajectories and their statistics for remotely entangled quantum bits," Phys. Rev. X **6**, 041052 (2016).

[12] A. N. Korotkov, "Quantum bayesian approach to circuit qed measurement with moderate bandwidth," Phys. Rev. A **94**, 042326 (2016).

[13] K. M. Gheri, K. Ellinger, T. Pellizzari, and P. Zoller, "Photon-wavepackets as flying quantum bits," Fortschritte der Physik **46**, 401 (1998).

[14] B. Q. Baragiola, R. L. Cook, A. M. Brańczyk, and J. Combes, "N-photon wave packets interacting with an arbitrary quantum system," Phys. Rev. A **86**, 013811 (2012).

[15] H. J. Carmichael, "Quantum trajectory theory for cascaded open systems," Phys. Rev. Lett. **70**, 2273 (1993).

[16] C. W. Gardiner, "Driving a quantum system with the output field from another driven quantum system," Phys. Rev. Lett. **70**, 2269 (1993).

[17] J. E. Gough, M. R. James, and H. I. Nurdin, "Quantum master equation and filter for systems driven by fields in a single photon state," in *Proceedings of the joint 50th IEEE Conference on Decision and Control and European Control Conference (CDC-ECC)* (2011) pp. 5570–5576.

[18] J. E. Gough, M. R. James, H. I. Nurdin, and J. Combes, "Quantum filtering for systems driven by fields in single-photon states or superposition of coherent states," Phys. Rev. A **86**, 043819 (2012).

[19] H. T. Song, G. F. Zhang, and Z. R. Xi, "Continuous-mode multiphoton filtering," SIAM Journal on Control and Optimization **54**, 1602 (2016).

[20] J. E. Gough, M. R. James, and H. I. Nurdin, "Quantum trajectories for a class of continuous matrix product input states," New Journal of Physics **16**, 075008 (2014).

[21] C. W. Gardiner and P. Zoller, *Quantum noise* (Springer, 2004).

[22] F. Le Kien and A. Rauschenbeutel, "Propagation of nanofiber-guided light through an array of atoms," Phys. Rev. A **90**, 063816 (2014).

[23] T. Caneva, M. T. Manzoni, T. Shi, J. S. Douglas, J. I. Cirac, and D. E. Chang, "Quantum dynamics of propagating photons with strong interactions: a generalized input–output formalism," New Journal of Physics **17**, 113001 (2015).

[24] K. Lalumière, B. C. Sanders, A. F. van Loo, A. Fedorov, A. Wallraff, and A. Blais, "Input-output theory for waveguide qed with an ensemble of inhomogeneous atoms," Phys. Rev. A **88**, 043806 (2013).

[25] R. L. Cook, *Continuous Measurement and Stochastic Methods in Quantum Optical Systems*, Ph.D. thesis, The University of New Mexico (2013).

[26] R. Dum, A. S. Parkins, P. Zoller, and C. W. Gardiner, "Monte carlo simulation of master equations in quantum optics for vacuum, thermal, and squeezed reservoirs," Phys. Rev. A **46**, 4382 (1992).

[27] R. van Handel, J. K. Stockton, and H. Mabuchi, "Modelling and feedback control design for quantum state preparation," J. Opt. B: Q. Semiclass. Opt. **7**, S179 (2005).

[28] G. J. Milburn and S. Basiri-Esfahani, "Quantum optics with one or two photons," Proceedings of the Royal Society of London A: Mathematical, Physical and Engineering Sciences **471** (2015).

[29] R. L. Hudson and K. R. Parthasarathy, "Quantum Ito's formula and stochastic evolutions," Commun. Math. Phys. **93**, 301 (1984).

[30] J. Gough, "Quantum Stratonovich calculus and the quantum Wong-Zakai theorem," J. Math. Phys. **47**, 113509 (2006).

[31] J. Combes, J. Kerckhoff, and M. Sarovar, "The SLH framework for modeling quantum input-output networks," arXiv:1611.00375 (2016).

[32] C. W. Gardiner and M. J. Collett, "Input and output in damped quantum systems: Quantum stochastic differential equations and the master equation," Phys. Rev. A **31**, 3761 (1985).

[33] A. Barchielli, "Direct and heterodyne detection and other applications of quantum stochastic calculus to quantum optics," Quantum Optics: Journal of the European Optical Society Part B **2**, 423 (1990).

[34] L. Bouten, R. V. Handel, and M. R. James, "An introduction to quantum filtering," SIAM Journal on Control and Optimization **46**, 2199 (2007).

[35] R. Loudon, *The quantum theory of light*, 3rd ed. (OUP Oxford, 2000).

[36] K. J. Blow, R. Loudon, S. J. D. Phoenix, and T. J. Shepherd, "Continuum fields in quantum optics," Phys. Rev. A **42**, 4102 (1990).

[37] R. Y. Chiao and J. C. Garrison, *Quantum Optics* (Oxford University Press, 2008).

[38] B. R. Mollow, "Quantum theory of field attenuation," Phys. Rev. **168**, 1896 (1968).

[39] M. W. Jack and M. J. Collett, "Continuous measurement and non-markovian quantum trajectories," Phys. Rev. A **61**, 062106 (2000).

[40] Moreover, $\rho_{m,n}(t)$ vanish for any index below zero. This way all of our superoperators are well defined.

[41] This differs from the Fock-state master equations in [14], where all diagonal matrices satisfy $\mathrm{Tr}[\rho_{n,n}(t)] = 1$.

[42] K. Jacobs and D. A. Steck, "A straightforward introduction to continuous quantum measurement," Contemporary Physics **47**, 279 (2006).

[43] P. Goetsch and R. Graham, "Linear stochastic wave equations for continuously measured quantum systems," Phys. Rev. A **50**, 5242 (1994).

[44] R. L. Cook, C. A. Riofrío, and I. H. Deutsch, "Single-shot quantum state estimation via a continuous measurement in the strong backaction regime," Phys. Rev. A **90**, 032113 (2014).

[45] H. M. Wiseman, "Quantum theory of continuous feedback," Phys. Rev. A **49**, 2133 (1994).

[46] G. J. Milburn, "Quantum measurement theory of optical heterodyne detection," Phys. Rev. A **36**, 5271 (1987).

[47] H. M. Wiseman, "SU(2) distribution functions and measurement of the fluorescence of a two-level atom," Quantum and Semiclassical Optics: Journal of the European Optical Society Part B **7**, 569 (1995).

[48] H. M. Wiseman, "Quantum trajectories and quantum measurement theory," J. Opt. B: Qantum and Semiclass. Opt. **8**, 205 (1996).

[49] A. Daeichian and F. Sheikholeslam, "Behaviour of two-

level quantum system drive by non-classical inputs," IET Control Theory and Applications **7**, 1877 (2013).
[50] P. D. Blocher and K. Mølmer, "How many atoms get excited when they decay?" arXiv:1702.08824 (2017).
[51] J. Dalibard, Y. Castin, and K. Mølmer, "Wave-function approach to dissipative processes in quantum optics," Phys. Rev. Lett. **68**, 580 (1992).
[52] The overall phase could be included in the wave packet $\xi(t)$, but we choose here to follow convention.
[53] B. Q. Baragiola, *Open Systems Dynamics for Propagating Quantum Fields*, Ph.D. thesis, University of New Mexico (2014).
[54] J. E. Gough and G. Zhang, "Generating nonclassical quantum input field states with modulating filters," EPJ Quantum Technology **2** (2015).
[55] T. Shi, D. E. Chang, and J. I. Cirac, "Multiphoton-scattering theory and generalized master equations," Phys. Rev. A **92**, 053834 (2015).
[56] S. Xu and S. Fan, "Input-output formalism for few-photon transport: A systematic treatment beyond two photons," Physical Review A **91**, 043845 (2015).
[57] C. Lee, C. Noh, N. Schetakis, and D. G. Angelakis, "Few-photon transport in many-body photonic systems: A scattering approach," Phys. Rev. A **92**, 063817 (2015).
[58] K. Koshino, "Single-photon filtering by a cavity quantum electrodynamics system," Phys. Rev. A **77**, 023805 (2008).
[59] T. Hong, H. Yang, H. Miao, and Y. Chen, "Open quantum dynamics of single-photon optomechanical devices," Phys. Rev. A **88**, 023812 (2013).
[60] W. Konyk and J. Gea-Banacloche, "Quantum multimode treatment of light scattering by an atom in a waveguide," Phys. Rev. A **93**, 063807 (2016).
[61] A. Roulet and V. Scarani, "Solving the scattering of n photons on a two-level atom without computation," New Journal of Physics **18**, 093035 (2016).
[62] P. P. Rohde, W. Mauerer, and C. Silberhorn, "Spectral structure and decompositions of optical states, and their applications," New Journal of Physics **9**, 91 (2007).
[63] A. R. R. Carvalho, M. R. Hush, and M. R. James, "Cavity driven by a single photon: Conditional dynamics and nonlinear phase shift," Phys. Rev. A **86**, 023806 (2012).
[64] S. R. Sathyamoorthy, L. Tornberg, A. F. Kockum, B. Q. Baragiola, J. Combes, C. M. Wilson, T. M. Stace, and G. Johansson, "Quantum nondemolition detection of a propagating microwave photon," Phys. Rev. Lett. **112**, 093601 (2014).
[65] A. Dabrowska, "Quantum filtering equations for systems driven by non-classical fields," arXiv:1611.06359 (2016).
[66] S. Basiri-Esfahani, C. R. Myers, J. Combes, and G. J. Milburn, "Quantum and classical control of single photon states via a mechanical resonator," New Journal of Physics **18**, 063023 (2016).
[67] Z. Dong, G. Zhang, and N. H. Amini, "Quantum filtering for multiple measurements driven by two single-photon states," in *2016 12th World Congress on Intelligent Control and Automation (WCICA)* (2016) pp. 3011–3015.
[68] Y. Liu, S. Shankar, N. Ofek, M. Hatridge, A. Narla, K. M. Sliwa, L. Frunzio, R. J. Schoelkopf, and M. H. Devoret, "Comparing and combining measurement-based and driven-dissipative entanglement stabilization," Phys. Rev. X **6**, 011022 (2016).
[69] J. Gough and M. R. James, "The series product and its application to quantum feedforward and feedback networks," IEEE Trans. Aut. Control **54**, 2530 (2009).

Appendix A: Temporal decomposition of Fock states

Here we expand on the temporal decomposition of Fock states within the wave packet $\xi(t)$. With respect to a time t, the wave packet creation operator decomposes as

$$B^\dagger_{t)}(\xi) = \int_{t_0}^{t} ds\xi_s b^\dagger(s) + \int_t^\infty ds\xi_s b^\dagger(s) \tag{A1}$$

$$= B^\dagger_{t)}(\xi) + B^\dagger_{[t}(\xi), \tag{A2}$$

where by definition $[B^\dagger_{t)}(\xi), B^\dagger_{[t}(\xi)] = 0$. Inserting this decomposition into Eq. (12) and expanding the product, a Fock state can be written

$$|n_\xi\rangle = \frac{1}{\sqrt{n!}} \sum_{k=0}^{n} \binom{n}{k} \left[B^\dagger_{t)}(\xi)\right]^k \left[B^\dagger_{[t}(\xi)\right]^{n-k} |\mathbf{0}\rangle \tag{A3}$$

with binomial coefficient

$$\binom{n}{k} \equiv \frac{n!}{k!(n-k)!}. \tag{A4}$$

The fact that Eq. (A3) does not factorize in time indicates temporal correlations between photons in the past and future time intervals. Applying a temporally decomposed wave packet creation operators to vaccum generates *unnormalized* Fock states over a time interval (chosen here to be the past interval $[t_0, t)$, for illustration)

$$|\overline{n}_{t)}\rangle = \frac{1}{\sqrt{n!}} \left[B^\dagger_{t)}(\xi)\right]^n |\mathbf{0}\rangle. \tag{A5}$$

They are unnormalized,

$$\langle\overline{n}_{t)}|\overline{n}_{t)}\rangle = [1 - w(t)]^n \tag{A6}$$

$$\langle\overline{n}_{[t}|\overline{n}_{[t}\rangle = [w(t)]^n. \tag{A7}$$

with

$$w(t) \equiv \int_t^\infty dt|\xi(t)|^2 \leq 1, \tag{A8}$$

because the division of $\xi(t)$ creates two temporal modes that are not individually square-normalized. Then, we can express Eq. (A3) as

$$|n_\xi\rangle = \sum_{k=0}^{n} \sqrt{\binom{n}{k}} |\overline{k}_{t)}\rangle \otimes |\overline{n-k}_{[t}\rangle. \tag{A9}$$

Using the normalizations, Eq. (A6), the past and future Fock states can be normalized,

$$|n_{t)}\rangle = [1 - w(t)]^{-\frac{n}{2}} |\overline{n}_{t)}\rangle \tag{A10}$$

$$|n_{t)}\rangle = [w(t)]^{-\frac{n}{2}} |\overline{n}_{t)}\rangle \tag{A11}$$

so that the temporal decomposition becomes

$$|n_\xi\rangle = \sum_{k=0}^{n} \sqrt{\binom{n}{k}} \sqrt{[1 - w(t)]^k [w(t)]^{n-k}} |k_{t)}\rangle \otimes |n - k_{[t}\rangle. \tag{A12}$$

1. Infinitesimal decomposition

Following the same procedure, we decompose the Fock state according to the three-interval temporal decomposition in Eq. (15). However, we choose to combine the past and future wave packet creation operators, only making the distinction with the current time interval $[t, t+dt)$. To this end we define $\overline{B}^\dagger_\xi \equiv B^\dagger_{t)}(\xi) + B^\dagger_{[t+dt}(\xi)$. Then Eq. (19) can be written,

$$\begin{aligned}
|n_\xi\rangle &= \frac{1}{\sqrt{n!}}\left[\xi(t)dB_t^\dagger + \overline{B}_\xi^\dagger\right]^n|\mathbf{0}\rangle \\
&= \frac{1}{\sqrt{n!}}\sum_{k=0}^{n}\binom{n}{k}\left(\xi(t)dB_t^\dagger\right)^k\left(\overline{B}_\xi^\dagger\right)^{n-k}|\mathbf{0}\rangle \\
&= \left[\frac{1}{\sqrt{n!}}\left(\overline{B}_\xi^\dagger\right)^n + \sqrt{n}\xi(t)dB_t^\dagger\frac{1}{\sqrt{(n-1)!}}\left(\overline{B}_\xi^\dagger\right)^{n-1}\right]|\mathbf{0}\rangle \\
&= |0_t\rangle\otimes|\overline{n}_\xi\rangle + \sqrt{n\,dt}\xi(t)|1_t\rangle\otimes|\overline{n-1}_\xi\rangle. \qquad \text{(A13)}
\end{aligned}$$

The third line follows from the Itō relation $dB_t^\dagger dB_t^\dagger = 0$, such that the only nonvanishing terms are $k=0$ and $k=1$, and in the last line we have used the definition of the infinitesimal single-photon state, Eq. (18). Equation (A13) is the relative-state decomposition in Eq. (20). The unnormalized Fock states $|\overline{n}_\xi\rangle = (1/\sqrt{n!})\left[\overline{B}_\xi^\dagger\right]^n|\mathbf{0}\rangle$ are defined on the joint past-future Hilbert space, $\mathcal{H}_{t)}\otimes\mathcal{H}_{[t+dt}$, which excludes the current interval. From Eq. (A13) the $|\overline{n}_\xi\rangle$ are clearly equivalent to the definition in Eq. (21). Their inner product, $\langle\overline{n}_\xi|\overline{n}_\xi\rangle = 1 - n\,dt|\xi(t)|^2$, can be worked out directly or by iteration as in Eq. (22).

Appendix B: Heisenberg-picture Fock-state SMEs

In some cases it proves useful to condition *operators*, rather than quantum states, on the continuous measurement record $\mathbf{R}$. In the mathematical quantum filtering literature [34], this is the preferred picture. Given the initial joint state $\rho_0\otimes\rho_{\text{field}}$, the conditional expectation of a system operator $X(t_0) = X\otimes I$ [34], is

$$\pi(X) \equiv \frac{1}{\Pr(\mathbf{R})}\text{Tr}_{\text{field}}\left[\rho_{\text{field}}C_{\mathbf{R}}^\dagger X C_{\mathbf{R}}\right]. \qquad \text{(B1)}$$

Conditional expectation values are calculated as $\mathbb{E}[X|\mathbf{R}] = \text{Tr}_{\text{sys}}\left[\rho_0\pi(X)\right]$. For input fields of the form of Eq. (88), the conditional operator in Eq. (B1) at time t is found by solving a set of coupled SMEs for the Fock-state conditional operators,

$$\pi_{m,n}(X) \equiv \frac{1}{\Pr(\mathbf{R})}\langle m_\xi|C_{\mathbf{R}}^\dagger X C_{\mathbf{R}}|n_\xi\rangle, \qquad \text{(B2)}$$

and then reconstructing $\pi(X)$ from the coefficients:

$$\pi(X) = \sum_{m,n} c^*_{m,n}\pi_{m,n}(X). \qquad \text{(B3)}$$

Note that $[\pi_{m,n}(X)]^\dagger = \pi_{n,m}(X^\dagger)$. The SMEs for $\pi_{m,n}[X]$ [18, 19] can be extracted directly from the Fock-state SMEs above using the cyclic property of the trace on each term. For example, multiplying a term $A\rho_{m,n}(t)B$ by X and taking the trace over system and field one can show,

$$\text{Tr}[A\rho_{m,n}(t)BX] = \text{Tr}_{\text{sys}}\left[\rho_0\pi_{n,m}(BXA)\right]. \qquad \text{(B4)}$$

Repeating this procedure on each of the Fock-state SMEs in Sec. III and identifying the terms in the system trace yields the SMEs in Heisenberg-form.

For continuous photon counting the Heisenberg-picture Fock-state SME is

$$\begin{aligned}
&d\pi_{m,n}(X) = \qquad \text{(B5)}\\
&dt\Big\{i\pi_{m,n}([H_{\text{sys}},X]) - \tfrac{1}{2}\pi_{m,n}(\{L^\dagger L,X\}_+) - \sqrt{m}\xi^*(t)\pi_{m-1,n}(S^\dagger LX) - \sqrt{n}\xi(t)\pi_{m,n-1}(XL^\dagger S)\Big\} + \Pr(J)\pi_{m,n}(X)\\
&+ dN\left(\frac{\pi_{m,n}(L^\dagger XL) + \sqrt{m}\xi^*(t)\pi_{m-1,n}(S^\dagger XL) + \sqrt{n}\xi(t)\pi_{m,n-1}(L^\dagger XS) + \sqrt{mn}|\xi(t)|^2\pi_{m-1,n-1}(S^\dagger XS)}{\Pr(J)} - \pi_{m,n}(X)\right)
\end{aligned}$$

with probability of photon detection

$$\Pr(J) = dt\sum_{m,n}c^*_{m,n}\text{Tr}_{\text{sys}}\Big[\rho_0\big\{\pi_{m,n}(L^\dagger L) + \sqrt{n}\xi(t)\pi_{m,n-1}(L^\dagger S) + \sqrt{m}\xi^*(t)\pi_{m-1,n}(S^\dagger L) + \sqrt{mn}|\xi(t)|^2\pi_{m-1,n-1}(I)\big\}\Big]. \qquad \text{(B6)}$$

For homodyne detection the Heisenberg-picture Fock-state SME is,

$$\begin{aligned}
d\pi_{m,n}(X) &= dt\Big\{i\pi_{m,n}([H_{\text{sys}},X]) + \pi_{m,n}(\mathcal{D}_L^\dagger[X]) \qquad \text{(B7)}\\
&+ \sqrt{m}\xi^*(t)\pi_{m-1,n}(S^\dagger[X,L]) + \sqrt{n}\xi(t)\pi_{m,n-1}([L^\dagger,X]S) + \sqrt{mn}|\xi(t)|^2\pi_{m-1,n-1}(S^\dagger XS - X)\Big\}\\
&+ d\mathcal{J}_\phi(t)\Big\{e^{i\phi}\big(\pi_{m,n}(LX) + \sqrt{m}\xi^*(t)\pi_{m-1,n}(S^\dagger X)\big) + e^{-i\phi}\big(\pi_{m,n}(XL^\dagger) + \sqrt{n}\xi(t)\pi_{m,n-1}(XS)\big) - K_\phi\pi_{m,n}(X)\Big\}.
\end{aligned}$$

where the adjoint-form Lindblad superoperator acting on X is $\mathcal{D}_L^\dagger[X] \equiv L^\dagger X L - \frac{1}{2}\big(L^\dagger L X + X L^\dagger L\big)$. The expected homodyne current is

$$K_\phi = \sum_{m,n} c^*_{mn} \mathrm{Tr}_{\mathrm{sys}}\Big[\rho_0\big\{\pi_{m,n}(e^{-i\phi}L + e^{i\phi}L^\dagger) + e^{i\phi}\sqrt{n}\xi(t)\pi_{m,n-1}(S) + e^{-i\phi}\sqrt{m}\xi^*(t)\pi_{m-1,n}(S^\dagger)\big\}\Big]. \tag{B8}$$

The Heisenberg-form SME for heterodyne detection follows straightforwardly from the homodyne SME in analogy with Eq. (80)

In each case, the SME for conditional operator $\pi_{m,n}(X)$ includes terms that couple to other conditional system operators, *e.g.* $\pi_{m-1,n}(S^\dagger X L)$, whose SMEs must be also solved simultaneously.